Application of LiDAR differencing to assess sediment load in the upper Waipaoa River, 2005 to 2019

BJ Rosser KE Jones

GNS Science Consultancy Report 2021/102
September 2022

DISCLAIMER

This report has been prepared by the Institute of Geological and Nuclear Sciences Limited (GNS Science) exclusively for and under contract to Gisborne District Council. Unless otherwise agreed in writing by GNS Science, GNS Science accepts no responsibility for any use of or reliance on any contents of this report by any person other than Gisborne District Council and shall not be liable to any person other than Gisborne District Council, on any ground, for any loss, damage or expense arising from such use or reliance.

Use of Data:

Date that GNS Science can use associated data: September 2022

BIBLIOGRAPHIC REFERENCE

Rosser BJ, Jones KE. 2022. Application of LiDAR differencing to assess sediment load in the upper Waipaoa River, 2005 to 2019. Lower Hutt (NZ): GNS Science. 55 p. Consultancy Report 2021/102.

CONTENTS

FIGURES

TABLES

APPENDICES

APPENDIX FIGURES

APPENDIX TABLES

EXECUTIVE SUMMARY

The 2205 km^2 Waipaoa River catchment drains from the Raukumara Ranges out to sea just south of the city of Gisborne. It is well known within New Zealand and internationally for its spectacular rates of landscape erosion, high sediment load and consequent rapid aggradation of the riverbed level in historic times (Marden et al. 2008; Kuehl et al. 2016; Gomez and Rosser 2018). Reforestation of the upper Waipaoa River catchment since 1960 has successfully reduced sediment loads from mass movement erosion in the highly erodible terrain (Marden et al. 2014) and, since the mid-1990s, has led to a reduction in the rate of bed-level rise (aggradation) in the headwater reaches (Gomez et al. 2003; Peacock and Marden 2019). However, riverbed levels continued to rise, and significant recovery of the river channel further downstream was considered unlikely for decades to centuries (Kasai et al. 2005). Analysis of cross-section data in the upper Waipaoa River reaches (Peacock and Marden 2019) suggests that the Waipaoa mainstem may now be showing signs of incising through these aggradational deposits in the channel network.

Gisborne District Council acquired airborne LiDAR data for the whole Gisborne region between 2019 and 2020. LiDAR was also acquired for parts of the Waipaoa River catchment in 2005. LiDAR differencing was performed by subtracting the 2019 LiDAR DEM from the 2005 LiDAR DEM to derive the change in elevation between the two surfaces. This allowed us to precisely quantify changes in riverbed elevation and channel morphology between 2005 and 2019 for the upper Waipaoa River channel and estimate rates of net sediment transfer through the study reaches. From 2005 to 2019, -2,291,000 m^3 of riverbed material was removed from the study reach and 859,000 m^3 was deposited. This gives an overall net loss of sediment from the study reach of -1,432,200 m^3, or an average of -102,000 m^3/yr, equivalent to 185,600 t/yr.

High rates of sediment generation and supply from the upper Waipaoa catchment caused riverbed aggradation over the length of the Waipaoa River in the historic period 1905–1996. Elevation changes in the Waipaoa and Te Weraroa rivers derived from differencing of LiDAR DEMs from 2005 and 2019 show that channel incision is now the dominant trend in these reaches. Channel incision was initiated in the headwater reaches and proceeded downstream at least as far as the confluence with the Waingaromia River. This suggests that the river is responding to the reduction in sediment supply due to erosion control efforts in the headwater catchments and that reforestation has been successful at reducing the sediment supply to the Waipaoa River. The implication of the transition from aggradation to degradation in the headwater reaches is that the dominant sediment source has switched from hillslope flux to sediment stored in beds of rivers and alluvial fans, as well as the sediment supplied from ‘badass gullies’ that are too big to be controlled by reforestation.

LiDAR differencing has allowed relatively precise quantification of the net change in sediment storage in the study reaches between 2005 and 2019, but the volumes represent a minimum rate of sediment transport and do not account for fluctuations in the rate of aggradation or degradation. Repeat LiDAR surveying is a highly practical methodology for determining net volumetric change in riverbed, floodplain and other valley deposits at the catchment scale (tens to hundreds of kilometres), with a relative error of only a few percent (given ~±10–25 cm vertical precision). LiDAR and cross-section analysis produced similar estimates of sediment storage volume changes; however, due to the amount of averaging in the calculation of sediment storage volume changes with cross-sections, LiDAR differencing is undoubtedly more accurate. Nevertheless, the length of record and regularity (both in time and space) of cross-section surveys in the Waipaoa River mean that the response of the river to both an increase and decrease in sediment supply over last 58 years is very well documented (Gomez et al. 2003, 2006, 2009; Tunnicliffe et al. 2018).

1.0 INTRODUCTION

The Waipaoa River drains from the Raukumara Ranges out to sea just south of Gisborne. It is well known within New Zealand and internationally for its spectacular erosion rates, high sediment load and consequent rapid aggradation of the riverbed level in historic times (Marden et al. 2008; Kuehl et al. 2016; Gomez and Rosser 2018; Figure 4.1).

Reforestation of the upper Waipaoa River catchment by the planting of the Mangatu Forest since 1960 has successfully reduced sediment loads from gullies, earthflow and landslides in the highly erodible terrain (Marden et al. 2014) and, since about the 1990s, has led to a reduction in the rate of bed-level rise (aggradation) in the headwater reaches (Gomez et al. 2003; Peacock and Marden 2019). However, bed levels have continued to rise in some reaches and tributaries of the upper Waipaoa, and significant recovery of the river channel further downstream was considered unlikely for decades to centuries (Kasai et al. 2001, 2005). In the context of geomorphic systems, 'recovery' refers to the time required for re-equilibration and return to a characteristic form following disturbance (Chorley 1962; Brierly and Fryirs 2000; Fryirs and Brierly 2000, 2012), such as an increase in sediment supply. Recent analysis of cross section data in the upper Waipaoa River reaches (Peacock and Marden 2019) suggests that the Waipaoa mainstem may be beginning to show signs of incising through the aggradational deposits stored in the channel network, reversing the historical trend of rapid aggradation in these channels (signs of recovery/relaxation following sediment inputs from about the 1930s).

The high rates of sediment generation and supply from the upper Waipaoa catchment caused riverbed aggradation over the length of the Waipaoa River, including the lower reaches where the river meanders over the Poverty Bay Flats (Peacock et al. 2009; Gomez et al. 2007). Over the last 50 years, the high suspended sediment load, largely generated by erosion in the upper Waipaoa, contributed to a narrowing of bankfull width by 23% and a reduction in bankfull cross-section area by 22% in these reaches, brought about by sedimentation on the river banks and aggradation of the bed (Gomez et al. 2007). The sedimentation has caused a 10% reduction in the Waipaoa River Flood Control Scheme capacity (Peacock 1991), prompting Gisborne District Council (GDC; 2020) to instigate a project to raise flood stopbank levels in 2018 (Peacock et al. 2009; https://www.gdc.govt.nz/council/major-projects/waipaoa-river-flood-control-scheme). Being able to quantify the trajectory of the fluvial system and current rate of sediment supply from the upper Waipaoa catchment is critical in order to identify risks to the Waipaoa Flood Control Scheme associated with further potential sedimentation.

Monitoring of sediment storage flux using cross-sections been conducted on the Waipaoa River since 1948. LiDAR (Light Detection and Ranging) is a remote sensing tool that uses laser pulses to generate large amounts of highly accurate topographic terrain data that has the potential to monitor geomorphic change when repeat surveys are performed (Lane et al. 2003; Wheaton et al. 2010). Digital elevation models (DEMs) built from these surveys can be used to produce DEMs of difference (DOD) or difference models that can be used to estimate the net change in sediment storage and the morphological sediment budgets (Wheaton et al. 2010). Typically, in fluvial geomorphology, repeat river planform or cross-section surveys have been used to estimate sediment transport due to the difficulties associated with measuring bedload transport directly (Gomez 1991). DODs have been shown to reduce some of the uncertainties associated with sediment volume estimates from these traditional methods (Fuller et al. 2003; Wheaton et al. 2010) and have been used to interpret geomorphic processes, such as channel scour and fill, and estimate bedload sediment transport rates (Wheaton et al. 2010; Williams 2012).

In New Zealand, LiDAR differencing has been used widely to interpret landscape change, including surface deformation from large earthquakes (Duffy et al. 2013; Beavan et al. 2012), geomorphic impacts associated with debris flows on Mt Tongariro (Proctor et al. 2014) and lahar on Mt Ruapehu (Proctor et al. 2010). LiDAR differencing was used to map the distribution and volumes of landslides (Massey et al. 2018, 2020; Bernard et al. 2021) triggered by and to assess coastal uplift associated with the M7.8 2016 Kaikōura earthquake (Clark et al. 2017). LiDAR differencing has been used in the fluvial setting to identify sediment pathways and debris distribution from the 2005 Matatā debris flow (Bull et al. 2010) and to estimate sediment transport in a large gravel-bed river (Lane et al. 2003).

DODs obtained from ground-based LiDAR (or terrestrial laser scanning) have been used to develop morphological sediment budgets for the Tarndale Gully in the Waipaoa catchment (Taylor et al. 2018). Fuller and Marden (2010, 2011) used DODs constructed from RTK-GPS surveys, and Fuller et al. (2020) used drone-based Structure from Motion techniques to monitor the patterns and changes in connectivity and the rate of erosion and deposition on the Tarndale fan. Tunnicliffe et al. (2018) and Leenman and Tunnicliffe (2018) successfully used drone-based Structure from Motion techniques to monitor sediment erosion, deposition and storage in the adjacent Waiapu catchment.

By utilising the latest LiDAR captured for the upper Waipaoa catchment in 2019 and comparing it to the 2005 LiDAR, this project aims to quantify changes in sediment accumulation and storage in the upper Waipaoa River and to quantify the net sediment supply rate from the upper Waipaoa catchment to the lower reaches (including the Waipaoa River Flood Control Scheme) over a 14 year period. Sediment volume estimates derived from the LiDAR differencing results will also be compared to the results derived from traditional river cross-section surveys carried out by GDC over the same period (Peacock and Marden 2019) to determine if LiDAR differencing is a viable method to quantify sediment loads in other rivers in the Gisborne region.

2.0 BACKGROUND TO PROJECT

As part of the New Zealand Government's Provincial Growth Fund, GDC acquired airborne LiDAR data for the whole Gisborne region between 2019 and 2020. LiDAR was also acquired for parts of the Waipaoa River catchment, including the upper Waipaoa and Waipaoa River Flood Control Scheme, in 2005. GDC is exploring ways to maximise the value of its investment in capturing airborne LiDAR and wants to assess the potential to use large-scale LiDAR differencing to assess the environmental risks (most notably, enhanced risk of flooding) associated with changing sediment supply to the Waipaoa River Flood Control Scheme. LiDAR differencing at the catchment scale may hold particularly good potential for detecting sites of anomalously high sediment yield, leading to improved capacity for focused management interventions. GDC has identified that the results generated from this project will contribute to the following areas of GDC work:

1. Understanding the sediment fluxes within the river system and identifying potential risks to the Waipaoa Flood Control Scheme associated with changing sediment supply rates.
2. Supporting flood hazard modelling for the Poverty Bay Flats.
3. Improving GDC's understanding of accretion and depletion of sediment on the beaches between the Waipaoa River and Gisborne City, which will help inform ongoing decision-making and long-term risk in this high-use environment under climate change.
4. Providing tools to allow for the application of LiDAR differencing in vulnerable catchments.
5. Providing a measure of the success of the Erosion Control funding programme in the mitigation of erosion and sediment losses in the Waipaoa Catchment.

3.0 PROJECT OBJECTIVES

The objectives for the Envirolink project are to:

- Undertake LiDAR differencing for the upper Waipaoa River (upstream of Whatatutu) using LiDAR collected by GDC in 2005 and 2019 to identify the spatial distribution of aggradation and degradation in the active river channel.
- Calculate the change in sediment volume in the channel system upstream of Whatatutu over the 14-year timespan.
- Compare channel aggradation and degradation rates to those calculated with cross-section surveys carried out by GDC over the same time-span.
- Determine if LiDAR differencing is a viable method for calculating medium-term sediment supply and storage rates in Gisborne District rivers (where repeat LiDAR is available).

4.0 STUDY AREA

The Waipaoa River catchment is located on the East Coast of the North Island and drains a 2205 km^2 catchment from the Raukumara Ranges of East Cape into Poverty Bay, just south of Gisborne (Figure 4.1). The Waipaoa River has a specific suspended sediment yield of 6800 t/km^2/yr and delivers 15 Mt of sediment into Poverty Bay each year, which equates to around 13% of the entire North Island sediment yield (Hicks et al. 2000). The majority of this sediment is suspended sediment, and only 1% of the total yield is estimated to be transported as bedload (Gomez et al. 2001). Average annual rainfall is 1000 mm/yr at the coast and ranges to >2500 mm/yr in the upper catchment (Thompson 1987). The mean annual discharge measured at Kananaia (Te Karaka) is 35 m^3/s, mean annual flood is approximately 1000 m^3/s and the largest flood on record of 4000 m^3/s was recorded during Cyclone Bola, 1988 (Hicks et al. 2004).

The study area consists of a 28 km reach of the Waipaoa River that stretches from the confluence with Tikihore Stream in the headwaters (downstream from XS 67) to the confluence with Waingaromia River, near Whatatutu (XS 48) (Figure 4.1). The study area includes a 7.2 km reach of Te Weraroa Stream from near the confluence with Tarndale Gully (XS 72) to the Waipaoa River confluence. Two significant sediment sources, the Tarndale and Mangatu gullies (and their fans), were included in the analysis, as were the lower reaches of major tributaries that were captured by the 2005 LiDAR. The extent of the study area was limited by the extent of the 2005 LiDAR capture, which was restricted to the river channels and land 100–300 m adjacent to the river, so this analysis is focused on sediment volume changes in the river channels only.

The headwaters of the Waipaoa River catchment are characterised by deeply dissected river channels caused by rapid uplift of the Raukumara Ranges within the zone of active deformation associated with the Hikurangi Subduction margin (Moore and Mazengarb 1992). Headwater catchments are underlain by thrusted Cretaceous to Palaeocene mudstone and argillite and Upper Cretaceous sandstone and siltstone of the Mangatu and Tikihore formations (Black 1980; Mazengarb et al. 1991; Figure 4.2). The rocks of the upper Waipaoa catchment are part of a shear zone associated with the emplacement of the East Coast allochthon in early Miocene times (Mazengarb et al. 1991), are crushed and sheared and are highly susceptible to erosion (Gage and Black 1979). The lower reaches of the catchment are underlain by Miocene and Pliocene mudstone and sandstone of the Te Arai and Tokomaru formations (Mazengarb et al. 1991). Shallow landslides are the dominant erosion process in the Tertiary rocks, whereas large ‘badass gullies’ and earthflows are common in the crushed and fractured rocks of the headwater regions (Trustrum et al. 1999; Marden et al. 2018; Fuller et al. 2020). Gully erosion is the dominant sediment source in the Waipaoa catchment, where it accounts for 43% of the annual suspended sediment yield (Marden et al. 2008).

The river enters a narrow gorge at Waipaoa Station, approximately 2 km downstream from the Te Weraroa confluence, where the river has incised between high Pleistocene terraces and low hills that are underlain by Miocene mudstone and sandstone. The morphology of the river undergoes a marked change from a multi-thread braided channel to a single-thread meandering channel at the upstream end of the gorge. The gorge is coincident with the change in lithology from the Cretaceous sediments of the East Coast Allochthon to Miocene mudstone of the Te Arai Formation, and it likely formed as a result of the inherent differences in relative rock strength between the crushed and sheared rocks of the East Coast Allochthon and the *in situ* cemented Miocene Mudstone (Rosser 1997). The presence of the relatively more resistant bedrock has possibly prevented the river from widening and braiding through this

reach. The gorge opens up downstream at the lithological boundary between the mudstone and a melange formed during the emplacement of the East Coast Allochthon (Mazengarb et al. 1991; Mazengarb and Speden 2000). Downstream of the gorge, the river has incised between high Pleistocene terraces and low hills predominantly underlain by Miocene and Pliocene sediments (Te Arai and Tokomaru formations), but it exhibits a braided channel and considerably wider floodplain with various levels of Holocene and Recent river terraces adjacent to the river (Rosser 1997).

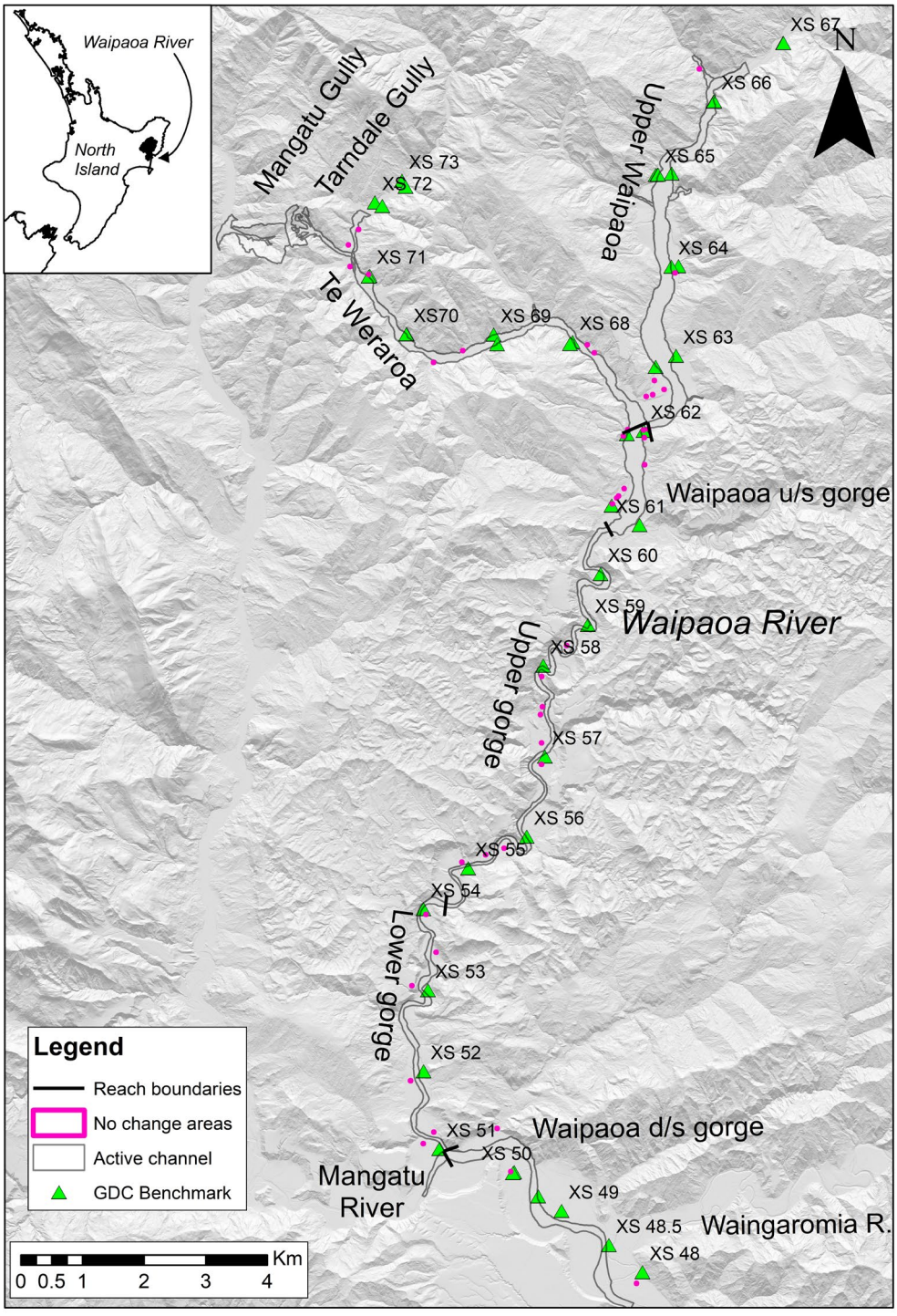

Figure 4.1 Study area, including the active channel of the Waipaoa and Te Weraroa rivers from the Tikihore confluence to near the confluence of the Waingaromia River, near Whatatutu. Also shown is the location of GDC cross-section benchmarks and the areas of no change used in the error analysis. The extent of the 2005 LiDAR is shown for reference. The background image is the 2019 GDC LiDAR Hillshade model.

The long-term trend of river incision in the headwaters was reversed over the historic period (post-1800) by a phase of rapid aggradation in the headwater channels that was triggered by wholesale conversion of the catchment from native forest to pasture (Allsop 1973; Gomez and Livingston 2012), which increased the area's susceptibility to erosion. A period of hillslope adjustment followed, resulting in the development of large gullies, earthflows, rotational slumps and shallow landslides that supplied large volumes of sediment to the river channels. The Waipaoa River and its tributaries have been aggrading in response to the increased sediment supply from about 1905 (Gage and Black 1979; Gomez et al. 1999, 2001). River channels in the upper Waipaoa River are braided, and steep alluvial fans occur at the confluence of tributaries in the upper reaches. Hillslopes in the upper Waipaoa are directly coupled to the river channel (Rosser 1997).

Reforestation of the headwater catchments began in the 1960s in an effort to slow the rate of erosion and sediment supply to the river channels (Allsop 1973). Reforestation has successfully reduced the rate of gully development (DeRose et al. 1998; Gomez et al. 2003; Marden et al. 2012, 2014); however, there are still many large gullies in the headwaters region that are too large to be controlled by reforestation (Marden et al. 2005; Herzig et al. 2011), so the sediment supply remains high (Fuller et al. 2020).

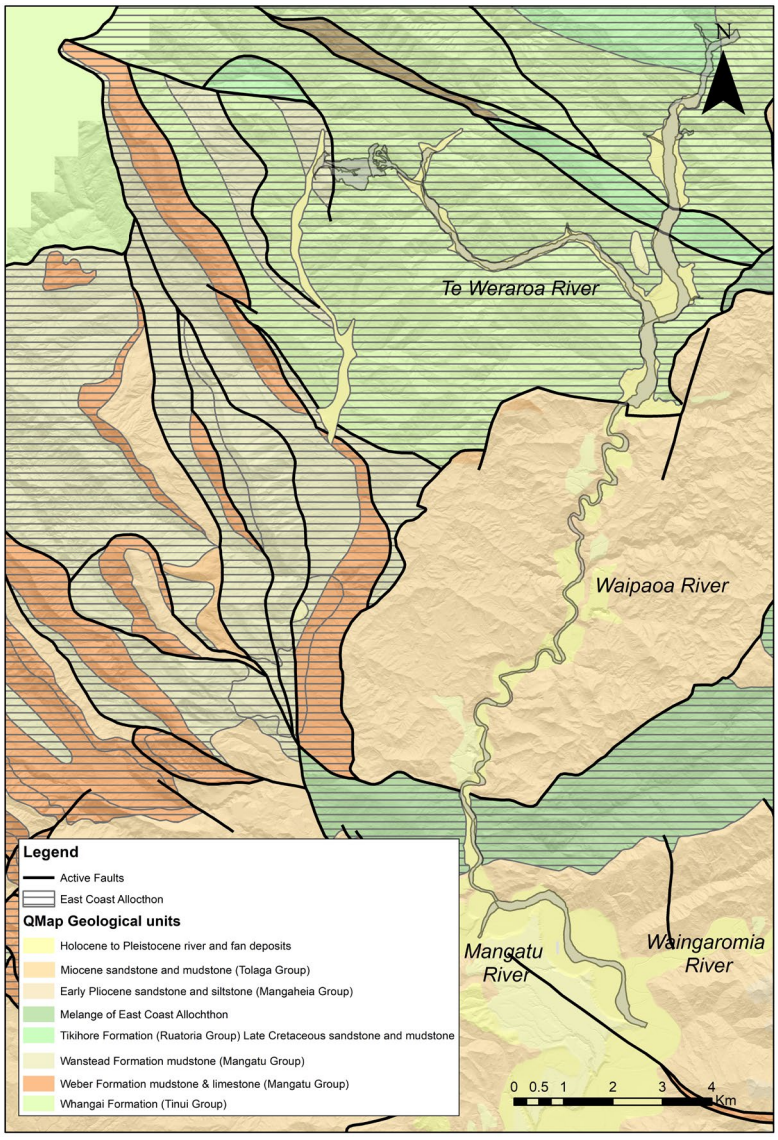

Figure 4.2 Simplified geology map of the upper Waipaoa River catchment. Data from 1:250,000 QMAP digital data (https://data.gns.cri.nz/geology/). The active channel of the study reach is shown in grey.

5.0 METHODOLOGY

5.1 Imagery and LiDAR

Aerial LiDAR and photography (at a resolution of 0.3 m) for the study area captured in 2005 and 2019 was supplied by GDC.

The 2005 Aerial LiDAR survey was flown by AAM Hatch Pty Limited of Australia. Airborne Laser Scanning (ALS) data was acquired from a fixed-wing aircraft between October and November 2005. The data was captured using NZGD1949 and projected in NZMG. The vertical datum was Gisborne Vertical Datum 1926. Vertical data accuracy was estimated to be ±0.15 m for derived points (interpolated from an ESRI terrain model) and horizontal <0.4 m for measured points (observed directly) (AAM Hatch 2006). Laser strikes were classified into 'ground' and 'non-ground' based upon algorithms tailored for terrain/vegetation combinations in the project area; however, ground definition may be less accurate in areas of thick vegetation or trees. The 2005 LiDAR dataset was captured with an average point separation of 0.8 m. The 2005 LiDAR point cloud was supplied by GDC in the NZMG1949 coordinate system and converted to NZTM/GD2000 map projection in ArcGIS.

The 2019 Aerial LiDAR survey was flown by Aerial Surveys Ltd between May 2019 and January 2020. The LiDAR survey was collected using an Aerial Surveys Optech Orion H300 LiDAR system. The 2020 LiDAR dataset was captured to a minimum of four points per square metre. The LiDAR point clouds were supplied in NZTM/GD2000 map projection and NZVD2016 and Gisborne 1926 vertical datum. The data was converted from NZGD2000 ellipsoidal heights into the local height system using the LINZ NZGeoid2016 separation model. The height accuracy of the ground-classified LiDAR points was validated using open land-cover survey check site data collected by Sounds Surveying Ltd. This was done by calculating height difference statistics between a TIN of the LiDAR ground points and the checkpoints. The mean error and standard deviation of the differences between ground LiDAR points and checkpoints were -0.027 m and 0.057 m, respectively (Aerial Surveys Ltd 2020). The data is freely available from the LINZ data service and opentopography.org.

Both 2005 and 2019 LiDAR point clouds were re-sampled to a common 1 m resolution DEM, and hillshade models were created in ArcGIS. The 1926VD version of both the 2005 and 2019 DEMs was used for differencing. The 2019 LiDAR data was re-processed by GNS Science to correct the LAS format and classification issues, in accordance with GDC feedback.

5.2 Definition of Active Bed and Reaches

The active bed width was defined for both the 2005 and 2019 surveys using interpretation of the LiDAR hillshade models and aerial photography captured with each survey (Figure 5.1). The cross-section survey data from GDC was also consulted to help define the active bed using left and right active bed (LAB, RAB) limits. The 'active bed' is defined as the actively re-worked (non-vegetated) alluvial surfaces in the river channel, such as bars and braid-plains, and represents the active sediment transport corridor (Peacock and Marden 2019). The active bed areas for 2005 and 2019 were combined to define the area of interest (recently active alluvial surface) over which the volume change calculations were performed. All change indicated by the LiDAR differencing within this alluvial zone was included.

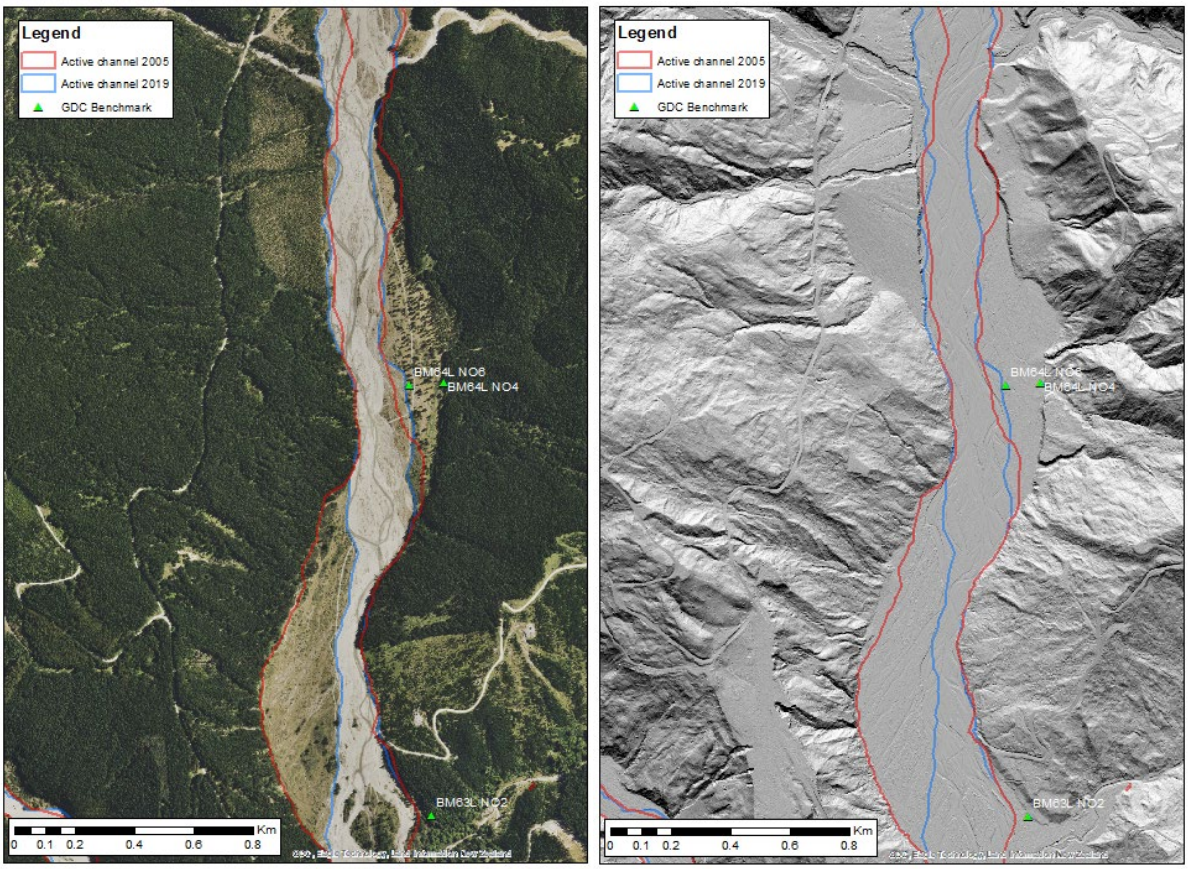

Figure 5.1 The active channel defined for the 2005 and 2019 surveys. The active channel area over which the volume change calculations were made was defined by the union of the 2005 and 2019 surveys to capture all areas of change over the 14-year period. The imagery and LiDAR shown is from the 2019 survey.

The active bed surface was divided longitudinally into river reaches that represent different river morphologies and/or relationships to significant sediment sources, such as tributaries and large gullies. The reaches used in this study are shown in Figure 4.1, and their morphological characteristics are listed in Table 5.1.

The width of the active bed over which the volume calculations were performed was measured in ArcGIS with the Measure tool, using the average of 10 channel widths measured perpendicular to the dominant channel thalweg (Table 5.1). Active bed width was also calculated for 2005 and 2019 for each reach by averaging the active bed widths using GDC cross-section survey data (from LAB and RAB distances). Average reach slope was calculated using mean bed level (MBL) data for GDC cross-sections by calculating the slope between each cross-section (elevation change/distance) and averaging for each study reach. Where no MBL data was available, slopes were calculated from the 2019 DEM.

Table 5.1 Reach characteristics and corresponding Gisborne District Council (GDC) cross-sections. Active channel width is the combined 2005 and 2019 active channel width over which the volume change calculations were performed.

Reach Name	Reach Length (km)	GDC XS	Average Slope (°)	Active Channel Width*		Morphology
				Average	Standard Deviation	
Upper Waipaoa	6.9	67–62	0.0101	173.5	80.4	Braided
Tikihore	0.5	-	0.0092	57.3	40.4	Braided
Matau	0.5	-	0.0082	67.7	41.6	Alluvial fan
Matakonekone	0.4	-	0.0233	26.4	12.4	Alluvial fan
Gully LB	0.3	-	0.0214	20.2	8.2	Alluvial fan
Te Weraroa U/s Tarndale	0.7	72–73	0.0212	94.0	7.1	Braided
Te Weraroa d/s Tarndale	6.5	68–71	0.0210	98.9	42.1	Braided
Oil Springs	0.3	-	0.0179	32.9	8.1	Alluvial fan
Waipaoa U/s gorge	1.9	61–62	0.0083	273.0	41.4	Braided
Upper gorge	9.6	60–54	0.0049	51.0	12.1	Single thread
Lower gorge	4.8	54–51	0.0036	61.3	26.5	Single thread
Mangatu River	0.8	119–120	0.0036	59.0	28.6	Braided
Waipaoa d/s gorge	4.8	48–51	0.0031	93.3	27.3	Braided
Tarndale Gully	0.4	-	41.395	683.0	-	Gully complex
Tarndale fan	1.0	-	0.0240	84.5	77.0	Alluvial fan
Mangatu Gully	0.9	-	37.002	645.0	-	Gully complex
Mangatu fan	0.9	-	0.0257	110.2	154.9	Alluvial fan

* Average of upper and lower fans.

The Tarndale Gully and Mangatu Gully were treated separately. Gully extents were defined by interpretation of the 2019 LiDAR hillshade model and aerial photography, and both gullies were divided into broad process zones representing active gully erosion and deposition on the fan (Figure 5.2). Tarndale Gully was further subdivided into different sub-catchments and process zones, as per Taylor et al. (2018). For this study, areas outside the active gully complex were not included in the volume calculations.

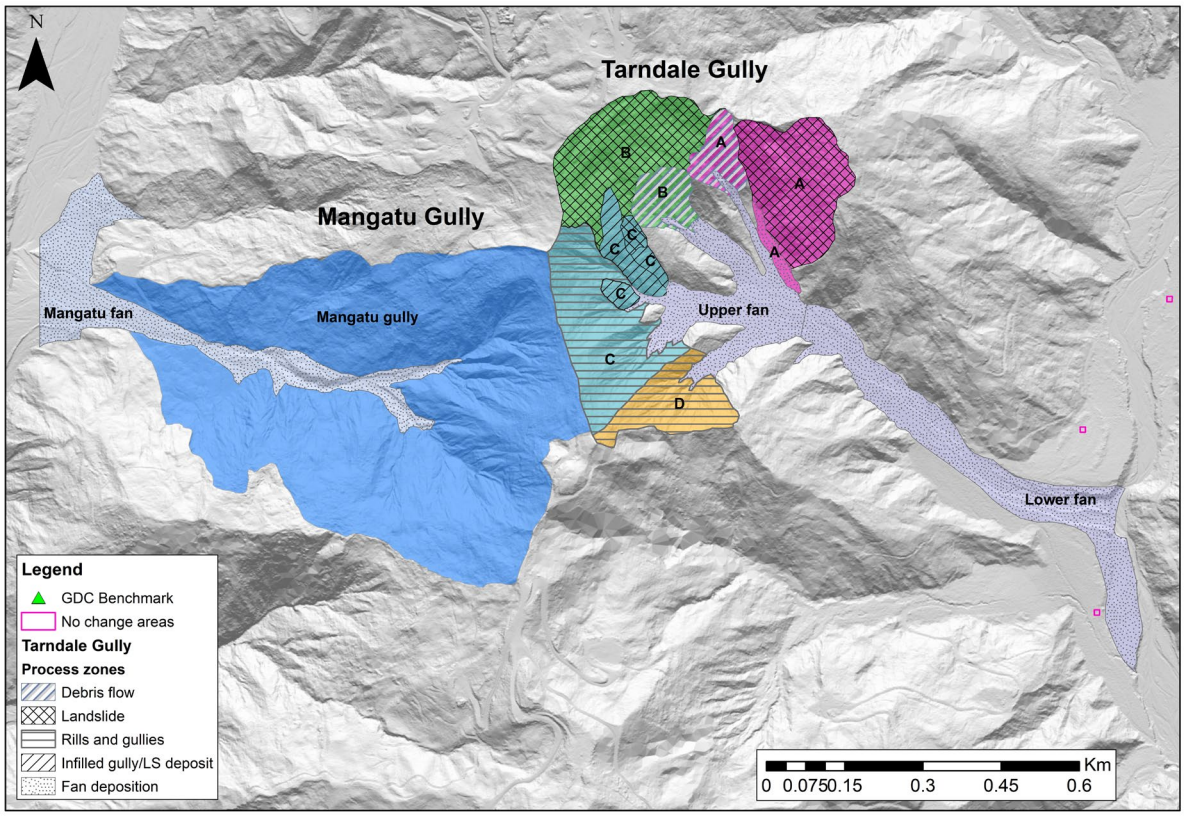

Figure 5.2 Mangatu Gully and Tarndale Gully process zones and sub-catchments (A–D) used for volume change calculations. The location areas of no-change grids used in the error analysis are also shown.

5.3 LiDAR Differencing and Volume Calculations

Changes in riverbed elevation and channel morphology can be precisely quantified by comparing the 2005 and 2019 LiDAR data to map the spatial distribution of bed-level change, as well as identifying which parts of the river are aggrading (or storing gravel) and which parts are degrading (loss of sediment from the reach). LiDAR differencing was performed by subtracting the 2019 LiDAR DEM from the 2005 LiDAR DEM to derive the change in elevation between the two surfaces for each 1 x 1 m raster cell. A positive change represents a net rise in bed level (or aggradation) over the 14-year period, and a negative change represents a drop in riverbed level (or degradation/incision). The elevation changes represent the net change between the two dates, and do not account for fluctuations in bed level between the surveys. The difference model was clipped to the alluvial surface, as defined above. The accuracy of the 2005 LiDAR was found to be lower (i.e. more noise was evident) in areas of forest or on steep slopes (AA Hatch 2006) but was better on areas of low slope with little or no vegetation, such as dry river floodplains. By only analysing the difference model within the recently active alluvial surface of the valley bottom, the areas of greater DEM uncertainty on steep vegetated slopes adjacent to the channels were avoided.

In ArcGIS, change in volume was calculated on a reach basis by summing the aggraded and degraded zones across each river reach using the sum function of the Zonal Statistics tool. The difference model was separated into positive vertical change (aggradation) and negative vertical change (degradation). The raster change models were then clipped to the combined alluvial extents, and the extent of volume calculations was defined by the overlap between the 2005 and 2019 LiDAR surveys. LiDAR returns from water surfaces are neither consistent nor accurate, so data from inundated sections of river are masked, and a trendline along the river shore is generated. In a process known as ‘hydro-flattening’, a surface is then interpolated

across the river. This obscures the true bathymetry of the river, leading to some inaccuracies when comparing two alluvial surfaces that contain threads of active flow. In some sediment budgeting workflows, the hydro-flattened sections are isolated and a more conservative error term is used for wetted topography (J Tunnicliffe, pers. comm.). In this study, flow was captured at the lowest base flows in both surveys, and the broad wandering-to-braided morphology meant that the proportion of the alluvial surface occupied by water was very low.

The sum of sediment volumes aggraded (deposited) or degraded (eroded) were calculated separately for each reach. This change in sediment volume over a period of time, or sediment flux, can be used to derive morphological sediment budgets (Fuller et al. 2011).

5.3.1 Error Analysis

The accuracy of the LiDAR difference model is dependent on the alignment between each of the LIDAR DEM epochs (Taylor et al. 2018). The accuracy of the difference model was determined by comparing DEM elevations at sites with apparently unchanged surface topography (Taylor et al. 2018). These were typically areas of flat or gently sloping terrain, such as pasture, terraces or abandoned floodplain, that had not seen a change in vegetation over the study period. Areas of no change in the upper Waipaoa catchment in the Mangatu Forest were difficult to ascertain due to active gullies, landslides or earthflows, along with changes in vegetation such as logging or re-planting of exotic forest.

The mean elevation difference was calculated for 40 10 x 10 m grids distributed throughout the study area (Figure 4.1). Elevation differences are considered to principally be the result of alignment error arising between the DEMs. The mean error of the vertical difference in the 40 areas of no change was 0.095 m, and the standard deviation of the error was 0.106 m. The standard error of the difference model was thus determined to be ±0.106 m. This compares closely with the established LiDAR point accuracy (above) and is consistent with literature on the topographic precision of LiDAR (e.g. Wheaton et al. 2010). The difference model is not corrected for the positive mean error, and so the risk remains that the difference model may slightly over-estimate aggraded zones and slightly under-estimate degraded zones.

5.3.2 Sediment Generation from Bank Erosion and Streamside Landslides

Sediment sources within the active channel, such as bank erosion between 2005 and 2019, and erosion of alluvial fans were mapped using the LiDAR difference model and aerial photography. Sediment sources adjacent to the channel (not included in the combined active channel width) were also mapped using the LiDAR difference model and aerial photography. The volume of material eroded or deposited for each feature was calculated using Zonal statistics as a table function in ArcGIS. Each feature was classified into erosion type, whether it was part of the combined active channel or not. Volumes of sediment generated that were part of the combined active channel were included in the LiDAR differencing results, whereas volumes of sediment generated on slopes adjacent to the channel were not (so volumes were additional to the LiDAR differencing results).

5.3.3 Comparison to Gisborne District Council Cross-Section Surveys

Cross-section surveys have been carried out on the Waipaoa River since 1947 to monitor bed-level changes in response to concerns over the large amount of sediment entering the channel from erosion in the upper Waipaoa catchment (Peacock 1991). Cross-section benchmarks were established at one-mile (1610 m) intervals by the East Cape Catchment Board, and there is a near-continuous record of mean bed elevation records from these

cross-sections from 1947 to 2019 for the Waipaoa River and its main tributaries (Gomez et al. 2001). Most cross-sections were surveyed at regular intervals of 2–3 years, as well as after major flood events. The changes in mean bed levels between surveys have been used to estimate the volume of material stored or removed from a reach between each survey (Peacock 1991; Peacock and Marden 2019) to provide information on the sediment flux in Waipaoa River. The mean bed level at each cross-section was calculated as the weighted mean of the elevation over the active channel portion of the cross-section (XS).

To estimate the volume of sediment generated between successive surveys, the change in mean bed level (MBL) was multiplied by the channel area between two consecutive cross-sections (MBL change * average XS area * distance between XS) to derive a volume of sediment deposited (positive change) or eroded (negative change) in the intervening reach between survey dates (as per Griffiths 1979).

Peacock and Marden (2019) analysed the upper Waipaoa cross-section data from 1948 to 2019 to document the changes in mean bed elevation over time. GDC cross-section and mean bed-level data were provided for this project by Dave Peacock (pers. comm.). Sediment volume changes were calculated for the period 2005–2019 for the Waipaoa River using mean bed-level data from Peacock and Marden (2019). Mean bed levels and volume change calculations were made for Te Weraroa Stream using cross-section data provided by GDC using the same methodology as Peacock and Marden (2019).

To compare the sediment volume changes from the LiDAR differencing to those calculated by analysis of cross-section data, two study reaches were examined: one in the upper Waipaoa (XS 61–66) and one on Te Weraroa (XS 68–70/3). The active channel polygon and difference model were clipped to the same area covered by the cross-sections. In the upper Waipaoa, this encompassed a 7.93 km reach from just downstream of Tikihore Stream to just above the gorge. In Te Weraroa, a 4.42 km reach between Tarndale Gully and the confluence with Waipaoa River was selected. The volume of sediment deposited or eroded from the reach was calculated by LiDAR differencing, as above. Cross-section data for Waipaoa River reaches downstream from XS 61 were available but not analysed as part of this project, as these cross-sections were not surveyed in 2005 and 2019.

6.0 RESULTS

6.1 LiDAR Differencing

The LiDAR difference model shows the net vertical change in elevation between 2005 and 2019 for the Waipaoa and Te Weraroa active channel in the study reaches (Figure 6.1, with more detail in Appendix 1), and the vertical changes are summarised in Table 6.1. The results of the volume change calculations are shown in Table 6.2.

From 2005 to 2019, ~2,291,000 m^3 (range -2,587,400/-2,000,100 m^3 at ±1 standard deviation of the difference model error – see Table 6.2 for the range of aggradation and degradation values, taking into account the standard error of the difference model) of riverbed material was removed from the study reach, and ~859,000 m^3 was deposited. This gives an overall net loss of sediment from the study reach of ~-1,432,200 m^3, or an average of ~-102,000 m^3/yr (diff/14yrs) over the 14 years. Using a dry bulk density of Waipaoa riverbed material of 1.82 t/m^3 (Gomez et al. 2009), this equates to 185,640 t/yr.

Apart from the reach immediately upstream of the gorge, all reaches in the upper Waipaoa River and Te Weraroa Stream exhibited an unambiguous loss of bed material and showed a trend of net bed-level degradation or incision over the study period. Most of the major tributaries that were included in the LiDAR differencing area also showed degradation in their lower reaches at their confluences with the Waipaoa River. LiDAR differencing results for each reach are presented below. The detailed difference models for each reach are presented in Appendix 1.

Table 6.1 Mean net vertical change for each of the river reaches between 2005 and 2019 from LiDAR differencing. All heights are quoted in metres.

Reach	Net Mean Bed-Level Change	Standard Deviation	Maximum Aggradation	Maximum Degradation
Upper Waipaoa	-0.43	1.02	4.76	-11.19
Tikihore	-1.03	1.04	1.78	-7.23
Matau	-1.19	0.79	0.94	-4.82
Matakonekone	-1.79	1.37	2.77	-4.64
Gully LB	0.66	0.79	3.26	-1.64
TeW u/s Tarndale	-1.68	1.33	1.22	-8.41
TeW d/s Tarndale	-0.85	1.20	8.84	-10.55
Oil Springs	-1.31	0.69	2.78	-3.29
Waipaoa u/s gorge	0.36	0.26	3.70	-5.49
Upper gorge	0.10	0.59	7.78	-9.13
Lower gorge	0.05	0.51	5.93	-5.59
Mangatu	0.18	0.39	1.74	-4.88
Waipaoa d/s gorge	-0.20	0.42	3.56	-4.30

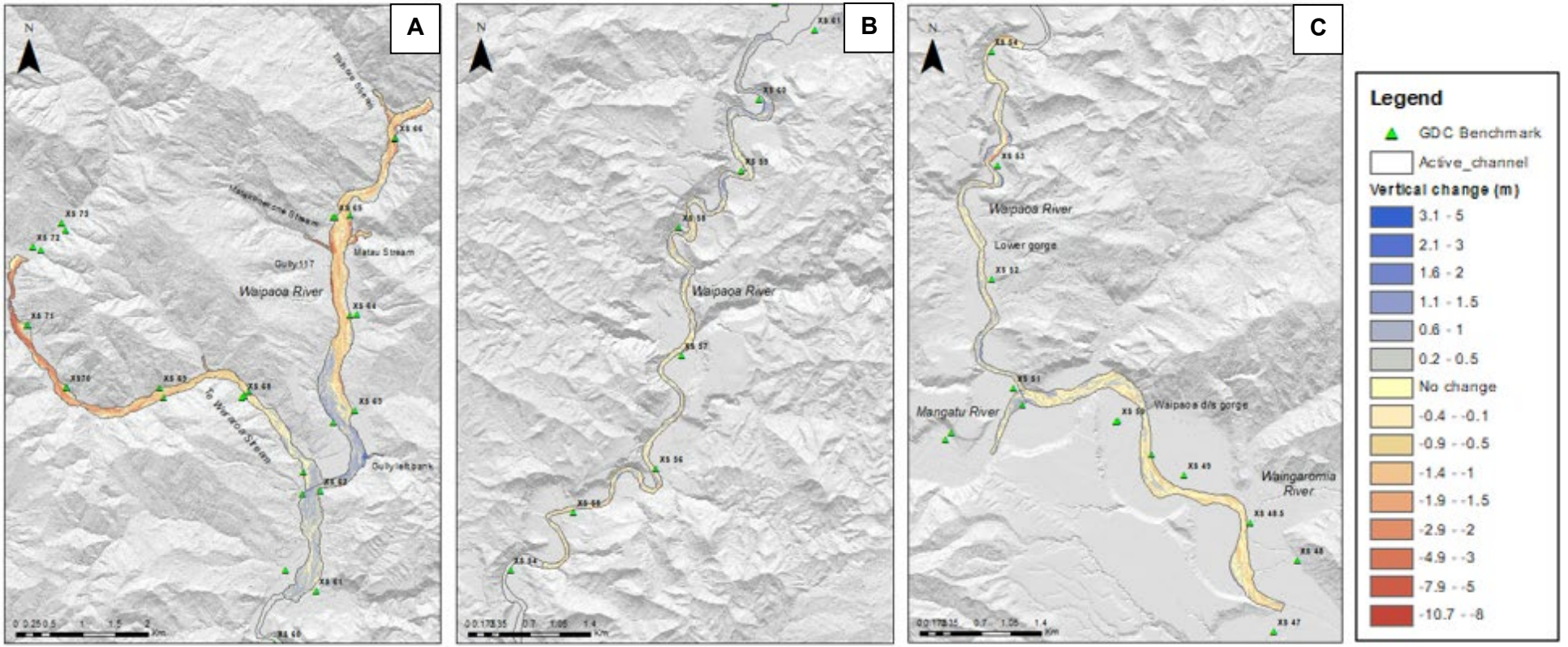

Figure 6.1 LiDAR difference models for the (a) upper Waipaoa, Te Weraroa and Waipaoa upstream of gorge; (b) upper gorge reach; and (c) lower gorge, Mangatu River and Waipaoa downstream of gorge. Reds and oranges represent erosion of sediment or degradation; blues represent sediment deposition or aggradation. Yellow indicates no change.

Table 6.2 Volumes of bed material deposited (aggradation) or eroded (degradation) from each of the river reaches between 2005 and 2019 from LiDAR differencing. All volumes are quoted in cubic metres.

Reach	Degradation	Aggradation	Degradation +1 σ	Degradation -1 σ	Aggregation +1 σ	Aggregation -1 σ	Net Volume Change	Dominant Process
Upper Waipaoa	-912,80	267,250	-811,450	-1,012,710	323,830	210,160	-644,820	Erosion
Tikihore	-40,680	2450	-37,530	-43,810	3120	1800	-38,220	Erosion
Matau	-38,350	240	-35,200	-41,510	400	90	-38,110	Erosion
Matakonekone	-26,650	530	-25,280	-28,020	650	400	-26,130	Erosion
Gully LB	-360	3800	-280	-470	4300	3330	+3450	Deposition
Te Weraroa d/s Tarndale	-787,160	78,660	-723,660	-855,900	107,290	55,270	-708,500	Erosion
Te Weraroa U/s Tarndale	-105,030	600	-99,120	-111,420	1520	180	-104,420	Erosion
Oil Springs	-11,360	180	-10,460	-12,260	230	150	-11,180	Erosion
Waipaoa u/s gorge	-5750	177,580	-3010	-11,240	227,510	130,400	+171,830	Deposition
Upper gorge	-104,780	170,650	-81,990	-133,400	219,140	128,000	+65,880	Deposition
Lower gorge	-61,110	81,690	-45,630	-81,230	109,560	58,470	+20,580	Deposition
Mangatu	-5010	16,260	-3090	-7470	21,040	12,010	+11,250	Deposition
Waipaoa d/s gorge	-193,040	59,260	-145,440	-247,970	87,160	38,700	-133,780	Erosion
Total Net Volume Change	**-2,291,330**	**859,160**	**-2,022,120**	**-2,587,410**	**1,105,750**	**638,950**	**-1,432,170**	**Erosion**

6.1.1 Waipaoa and Te Weraroa Rivers

Upper Waipaoa: There was a net loss of bed material sediment of ~-644,820 m^3 (see Table 6.2 for the ranges of aggradation and degradation values, taking into account the standard error of the difference model) from the upper Waipaoa reach over the study period (Table 6.2) and a corresponding drop in MBL of -0.434 m (Table 6.1). The dominant trend from 2005 to 2019 was degradation, and this persists downstream to near XS 63 (Figure A1.1). Downstream from XS 63, aggradation was the dominant process. A large lateral bar on the right bank that was active in 2005 but had stabilised and vegetated by 2019 marks the upstream extent of net aggradation. The maximum reduction in local elevation (-8 to -11 m) occurred between XS 64 and 65, where the river has trimmed the alluvial fans of Matakonekone Stream and Gully 117. All of the major tributaries feeding into this reach also incised in their lower reaches over the study period, apart from an actively eroding gully on the left bank, which formed an alluvial fan in the channel halfway between XS 62 and 63, causing 1.2–3.8 m of aggradation in the main stem. Average channel width (calculated using GDC cross-section data) declined from 118 to 113 m (-4.2 m) over the study period due to the stabilisation of several large bars, which allowed vegetation to colonise the bar surfaces.

Te Weraroa: There was a net loss of bed material from the Te Weraroa channel of ~-812,900 m^3 over the study period (u/s and d/s Tarndale combined). The Te Weraroa channel is now incising for most of its length, and bed degradation extends from upstream of Tarndale Gully to about 1 km upstream from the confluence with the Waipaoa River (Figure A1.2). MBL in the active channel decreased by -0.85 m (±1.2 m) in the reach below Tarndale, and maximum incision of around 9–10.5 m occurred where Te Weraroa Stream is confined by and has trimmed the edge of Tarndale fan, but the incision has been persistent in the Te Weraroa channel downstream of Tarndale fan, where there has been up to -4 to -5 m of channel incision (near XS 71). The amount of incision decreases to about -0.5 m at XS 68. Downstream of XS 68 to the confluence with the Waipaoa, there is slight aggradation of 0.1–0.3 m. The greatest aggradation occurred where landslide deposits and alluvial fans entered the channel. For example, about 175 m downstream from XS 68, a landslide deposited up to 8 m of material in the channel, and 860 m downstream from XS 68 is an alluvial fan from an active gully on the left bank.

From 2005 to 2019, the Te Weraroa active channel in the study reach narrowed by an average of -34.1 m, from 131.3 m to 97.2 m (from GDC cross-section data). The Te Weraroa channel exhibited the largest reduction in active channel width of all the study reaches. Several large lateral bars and fans stabilised over the study period and became vegetated.

Waipaoa upstream of gorge: This reach was dominated by aggradation, with an average net sediment gain of ~171,800 m^3 and an average vertical change of +0.36 m (±0.261 at 1 standard deviation). The only area that showed a loss of material (-4 to 5 m) was at a deposit of a landslide near XS 62 that was present in 2005 but had been eroded by 2019 (Figure A1.3).

A total volume of ~1,567,900 m^3 was supplied to this reach from the Te Weraroa and upper Waipaoa reaches over the study period, and ~171,800 m^3 was stored in that reach, with ~1,396,100 m^3 transferred to the gorge reach downstream. That means that 11% of the material supplied to this reach remained in storage and 89% of material was transferred downstream.

Upper and lower Waipaoa gorge: There was a small net increase in sediment storage in both upper and lower Waipaoa gorge reaches, with ~65,900 m^3 and ~20,600 m^3, respectively, being deposited in the gorge. Volumes of sediment build-up and incision were very similar (Table 6.2; Figures A1.4 and A1.5). The average change in riverbed elevation was +0.10 m (±0.58 m) in the upper gorge and +0.05 m (±0.51 m) in the lower gorge.

There was some evidence for slight channel narrowing in the upper gorge reach, where active channel width decreased slightly from 53.50 to 51.46 m. This is largely due to some large lateral bars that have become stabilised and vegetated over the study period (e.g. near XS 60 and downstream of XS 59). However, the lower gorge reach did not show any significant change in active channel width (66.85 to 66.37 m, -0.48 m).

~-1,396,100 m^3 of sediment was transferred to the gorge from the reaches upstream. Of this, ~86,500 m^3 was stored in the gorge reach and ~-1,309,600 m^3 transferred to the reaches below. Only 6% of material supplied to the gorge from upstream remains stored in the gorge, with 94% transferred to the lower reaches, confirming that the gorge reach is very efficient at moving sediment through, as suggested by Rosser (1997) and Peacock and Marden (2019).

Mangatu River: There was a small net gain in sediment of ~11,200 m^3 and slight aggradation of +0.18 m (± 0.39) in this very short reach (0.8 km) (included in the LiDAR differencing area) of the Mangatu River above the confluence with the Waipaoa River (Figure A1.6). There was no change in average channel width over the study period.

Waipaoa downstream of gorge: There was ~-193,000 m^3 of bed material eroded from this reach and ~59,300 m^3 was deposited, amounting to a net loss of bed material of ~-133,800 m^3. The MBL also declined by -0.20 m (± 0.42) (from LiDAR differencing) (an average rate of -13.92 mm/yr). The overall trend has evidently been degradation from 2005 to 2019. Four times as much material was removed from the reach than was deposited (despite 1.3 M m^3 material being supplied from upstream; Figure A1.6). Average channel width decreased by 4.6 m, from 94.9 to 90.3 m (mean width from XS data) from 2005 to 2019.

A minimum of ~1,309,600 m^3 was supplied to this reach from upstream (from the Mangatu and Waipaoa rivers), as well as the ~-133,800 m^3 that was eroded from this reach, meaning that ~1,443,400 m^3 of material was supplied to the downstream river reaches.

6.1.2 Sediment Generation from Bank Erosion and Streamside Landslides

Mapping of sediment sources adjacent to and along the active channel using LiDAR differencing indicates that ~-180,000 m^3 of material was supplied to the channel from bank erosion and streamside landslides (not included in differencing volumes of the active channel in Table 6.2) and that ~-263,000 m^3 of the sediment loss within the 2005–2019 active channel was due to bank erosion or streamside landslides. A breakdown of the sediment volumes from mass wasting processes for each reach is presented in Table 6.3. Of note is:

- ~197,000 m^3 of sediment was introduced to the channel from the erosion of alluvial fans in the upper Waipaoa reach.
- ~60,000 m^3 was supplied from streamside landslides in the upper Waipaoa reach (not included in volumes calculated for the active alluvial surface) (Figure 6.2).
- ~25,000 m^3 of sediment was derived from the erosion of alluvial fans in Te Weraroa reach.
- Nearly 100,000 m^3 was introduced to the channel from streamside landslides in the gorge reaches (not included in active channel), equivalent to ~7000 m^3/yr.

It is important to note that this material would be a mixture of bedload and suspended load (whereas the changes in sediment volume on the active channel bed is considered bedload). Additionally, the error analysis on the LiDAR difference model did not include slopes adjacent to the river, and thus uncertainty on bank erosion and streamside landslide volumes is likely to be underestimated. Nonetheless, these volume calculations give an indication of the scale of sediment sources along the study reaches.

Table 6.3 Volumes of sediment supplied to the channel from adjacent slopes and generated from different mass movement erosion types within the active channel from LiDAR differencing, 2005–2019.

Reach Erosion type	**Supplied to Channel (m^3)** (not included in active channel differencing volume)	**Within Active Channel (m^3)** (included in differencing volume)
Upper Waipaoa		
Bank erosion	-2980	-8530
Bank erosion – fan	-4150	-196,790
Gully	-1600	-
Streamside landslides	-58,460	-5060
Total	**-67,180**	**-210,380**
Te Weraroa		
Bank erosion	-	-6130
Bank erosion – fan	-16,490	-25,000
Gully	-4770	-
Streamside landslides	16,620	-
Total	**-4650**	**-31,130**
Waipaoa u/s Gorge		
Bank erosion	-	2050
Streamside landslides	-2480	-850
Total	**-2480**	**1200**
Upper Gorge		
Bank erosion	-3950	-10,270
Streamside landslides	-93,000	-7690
Total	**-96,960**	**-17,960**
Lower Gorge		
Bank erosion	-1500	-5770
Bank erosion – fan	-110	-
Landslide deposit	-	2150
Streamside landslides	-6670	-1140
Total	**-8280**	**-4760**
d/s Gorge		
Streamside landslides	-2980	-1000
Total	-2980	-1000
Grand Total	**-179,540**	**-263,030**

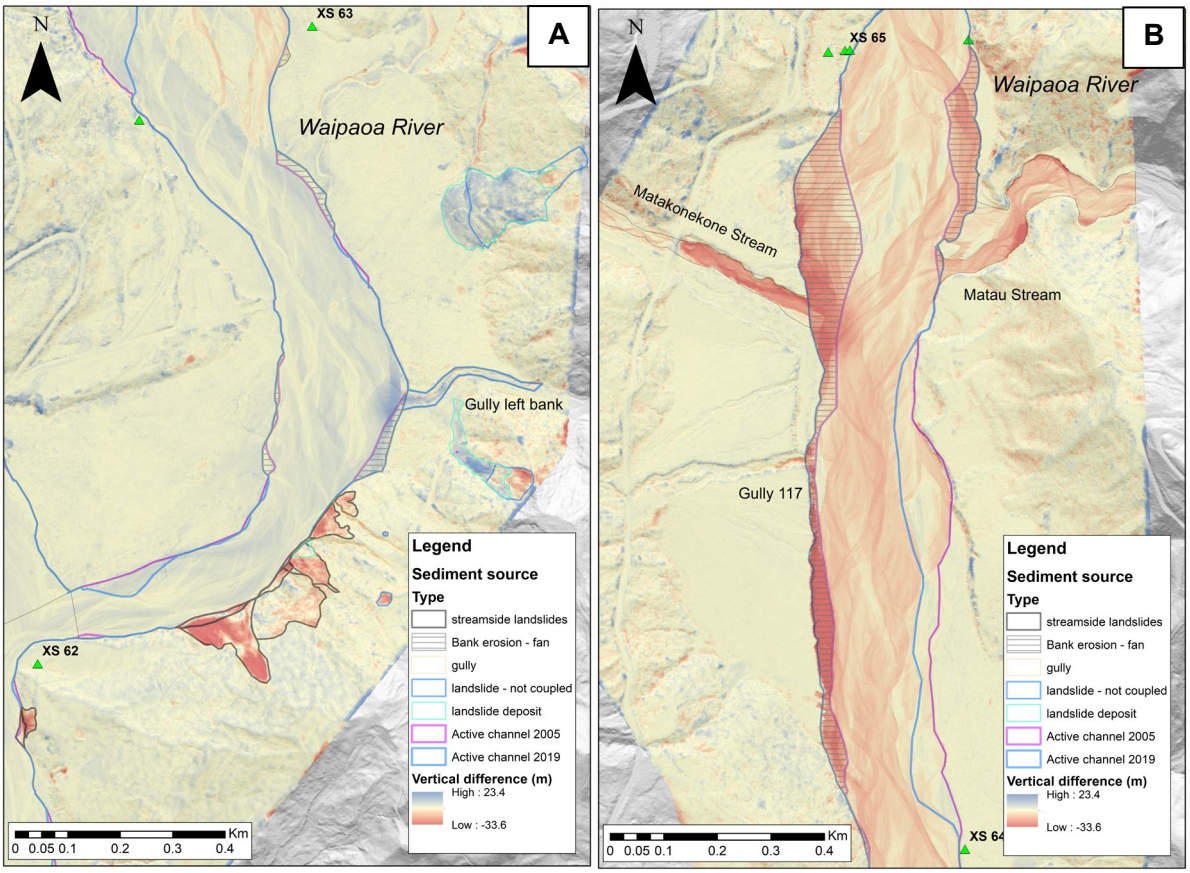

Figure 6.2 Examples of the unclipped LiDAR difference model in the upper Waipaoa reach (a) just upstream from the Te Weraroa Stream confluence and (b) at the confluence of Matakonekone and Matau streams, showing streamside landslides and erosion of fans identified by the differencing and the mapping of sediment sources for volume calculations.

6.1.3 Tarndale and Mangatu Gullies

Aerial photos taken in 2005 and 2019 illustrate the changes in vegetation and gully extent between the two LiDAR captures for the Tarndale and Mangatu gullies (Figure 6.3a and b), and the LiDAR difference model shows the net vertical surface change (Figure 6.3c). The results of the volume change calculations and elevation changes are shown in Tables 6.4 and 6.5, respectively. The location of Tarndale Gully sub-catchments and process zones used in the volume calculations are shown in Figure 5.2. The results of the LiDAR differencing are summarised as follows:

- From 2005 to 2019, a total net sediment volume of ~-1,007,300 m^3 (see Table 6.4 for standard-deviation-adjusted volumes) was removed from Tarndale Gully and ~212,500 m^3 was deposited on the fan. This means that ~-794,900 m^3 was delivered to Te Weraroa Stream from the Tarndale Gully complex.
- Using a bulk density of Tarndale fan material of 1.84 t/m^3 (De Rose et al. 1998), this equates to ~104,500 t/yr delivered to Te Weraroa Stream.
- Over the same timeframe, ~-1,265,600 m^3 of material was removed from Mangatu Gully and ~212,500 m^3 was deposited on the Mangatu fan (the part that was included in LiDAR differencing). This means that a minimum of ~-1,167,300 m^3 was delivered to the Mangatu River by the Mangatu Gully complex.
- Using a bulk density of Tarndale fan material of 1.84 t/m^3 (De Rose et al. 1998), this equates to ~153,421 t/yr delivered to Mangatu River from Mangatu Gully.

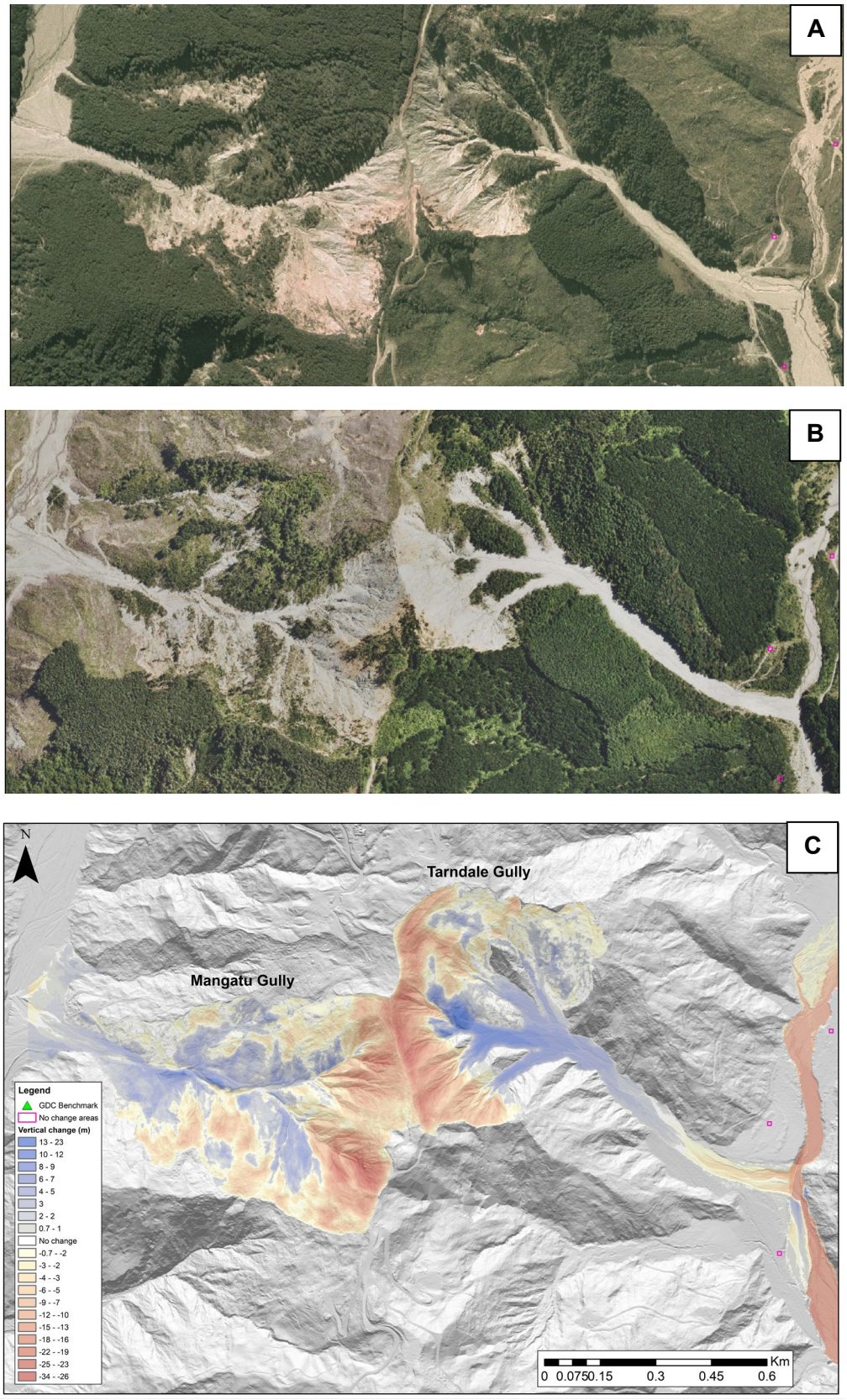

Figure 6.3 Tarndale and Mangatu gullies in (a) 2005 and (b) 2019, with (c) LiDAR differencing results.

Table 6.4 Volumes of bed material deposited (aggradation) or eroded (degradation) from each of the river reaches between 2005 and 2019 from LiDAR differencing. All volumes are quoted in cubic metres.

Catchment	Process Zone	Area (m^2)	Degradation	Aggradation	Degradation +1 σ	Degradation -1 σ	Aggradation +1 σ	Aggradation -1 σ	Net Change (m^3)
A	Debris flows	10,570	-26,530	970	-25,560	-27,560	1140	810	-25,570
A [1]	Landslide	43,000	-28,910	19,260	-26,160	-31,780	21,140	17,310	-9660
A [1]	Fan	3630	-240	2710	-130	-310	3050	2440	2470
B [1]	Landslide	47,180	-259,540	10,890	-255,230	-263,900	11,780	10,050	-248,650
B	Debris flows	11,700	-33,760	1220	-32,660	-34,890	1400	1060	-32,550
C	Rills and gullies	48,300	-620,870	760	-615,730	-626,020	940	600	-620,110
C	Landslide deposit	8840	-3620	50,080	-3400	-3850	50,840	49,340	46,460
C	Landslide deposit	2310	-10	14,740	-10	-20	15,000	14,490	14,730
C	Landslide	2360	-10,880	4	-10,620	-11,140	5	3	-10,880
C	Landslide deposit	2780	-370	10,630	-330	-420	10,890	10,360	10,250
D	Rills and gullies	23,540	-136,150	2300	-133,850	-138,480	2590	2030	-133,850
Tarndale fan	Upper fan	44,170	-590	219,580	-510	-690	224,350	214,820	219,000
Tarndale fan	Lower fan	64,880	-63,160	56,650	-60,230	-66,470	60,860	52,820	-6510
Tarndale Net Volume Change	-	-	**-1,184,650**	**389,790**	**-1,164,430**	**-1,205,510**	**403,990**	**376,140**	**-794,860**
Mangatu Gully [1]	Gully	365,280	-1,480,880	215,300	-1,453,220	-1,509,050	227,850	203,270	-1,265,580
Mangatu Fan [1]	Fan	64,960	-14,510	112,750	-13,320	-15,860	118,710	106,960	98,240
Mangatu Net Volume Change	-	-	**-1,495,380**	**328,050**	**-1,466,540**	**-1,524,900**	**346,560**	**310,220**	**-1,167,330**

[1] Areas not included in Taylor et al. (2018) calculations.

Table 6.5 Elevation changes on Tarndale and Mangatu gullies, 2005–2019.

Catchment	Area (m^2)	Vertical Elevation Change (m)					Volume (m^3)
		Min.	Max.	Range	Mean	Std. Dev.	
Tarndale A	57,080	-12.9	7.6	20.6	-0.6	1.9	-32,760
Tarndale B	58,873	-21.4	5.0	26.4	-4.8	5.3	-281,200
Tarndale C	64,560	-30.5	19.3	49.9	-8.7	9.6	-559,540
Tarndale D	23,547	-17.0	3.5	20.4	-5.7	4.0	-133,850
Tarndale upper fan	44,076	-3.1	12.5	15.7	5.0	2.9	219,000
Tarndale lower fan	64,820	-10.6	5.9	16.4	-0.1	2.5	-6510
Mangatu Gully	365,042	-33.6	8.6	42.2	-3.5	5.9	-1,265,580
Mangatu fan	64,848	-10.5	12.7	23.3	1.5	2.3	98,240

Comparison of the extent of the Tarndale and Mangatu gullies in 2005 and 2019 indicates that both gullies enlarged between 2005 and 2019 (Figures 6.3 and 6.4). The Tarndale Gully drainage divide moved west into the Mangatu Gully catchment by 18–20 m in catchment C and lowered by as much as 21 m. The head scarp in catchment D also retrogressed in a northwest direction up to 50 m (also into the Mangatu Gully catchment), and the surface lowered by as much as 20 m as a deep-seated landslide became active in this part of the gully complex. Mangatu Gully also enlarged in the southern corner by about 20–30 m and encroached into Tarndale catchment as gully processes became more active in that region of the gully.

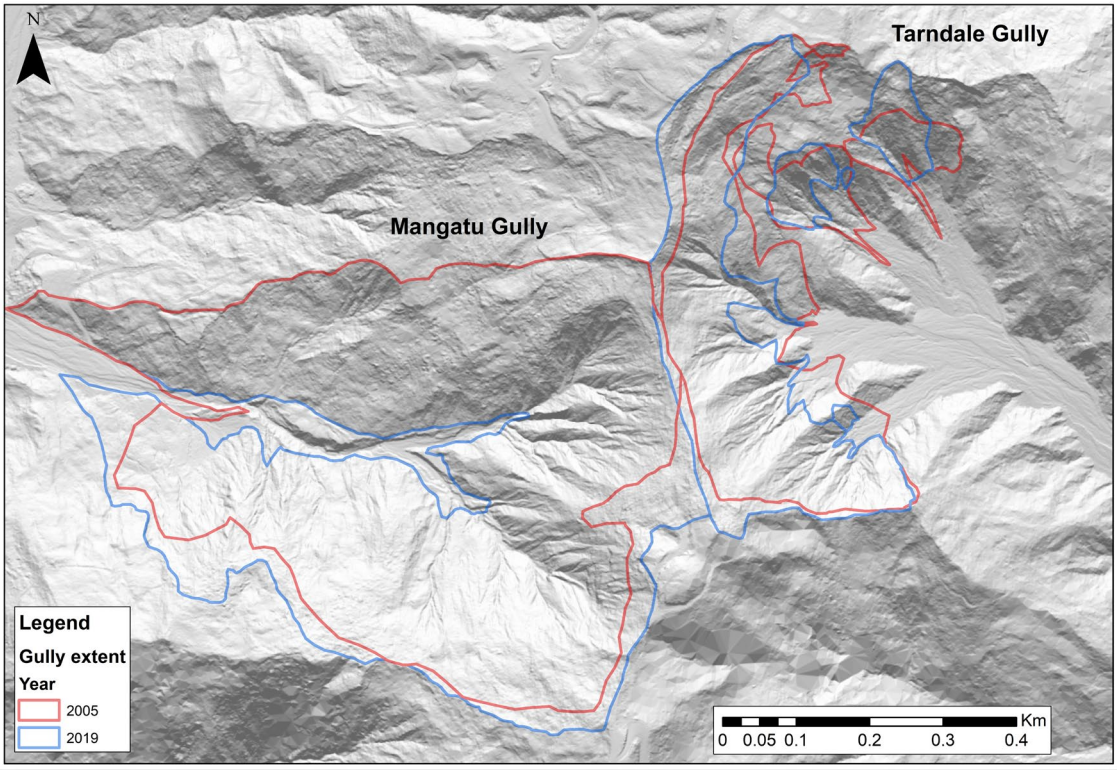

Figure 6.4 Extent of Tarndale and Mangatu gullies in 2005 and 2019, mapped using LiDAR and aerial photography for each year.

6.1.4 Comparison of LiDAR Differencing to Gisborne District Council Cross-Section Analysis

The LiDAR difference models for the two study reaches used to compare sediment volumes from the LiDAR differencing to those calculated by analysis of cross-section data are shown in Figure 6.5, and the changes in sediment volumes are shown in Table 6.6. Results of the volume change calculations from GDC cross-section data are shown in Tables 6.7 and 6.8. GDC cross-section data used in these calculations is presented in Appendix 2. The differences between the results from the two survey techniques are summarised as follows:

- The net volume change for Waipaoa XS 61–66 calculated from LiDAR differencing was -400,870 m^3 (-403,170/-398,570 m^3) and -308,700 m^3 from cross-section analysis. For this period, cross-section analysis **under-estimated** sediment volume change by 23%.
- The net volume change for Te Weraroa XS 68–71 calculated from LiDAR differencing was -618,900 m^3 (-572,680/665,120 m^3) and -1,021,450 m^3 from cross-section analysis. For this period, cross-section analysis **over-estimated** sediment volume change by 40%.

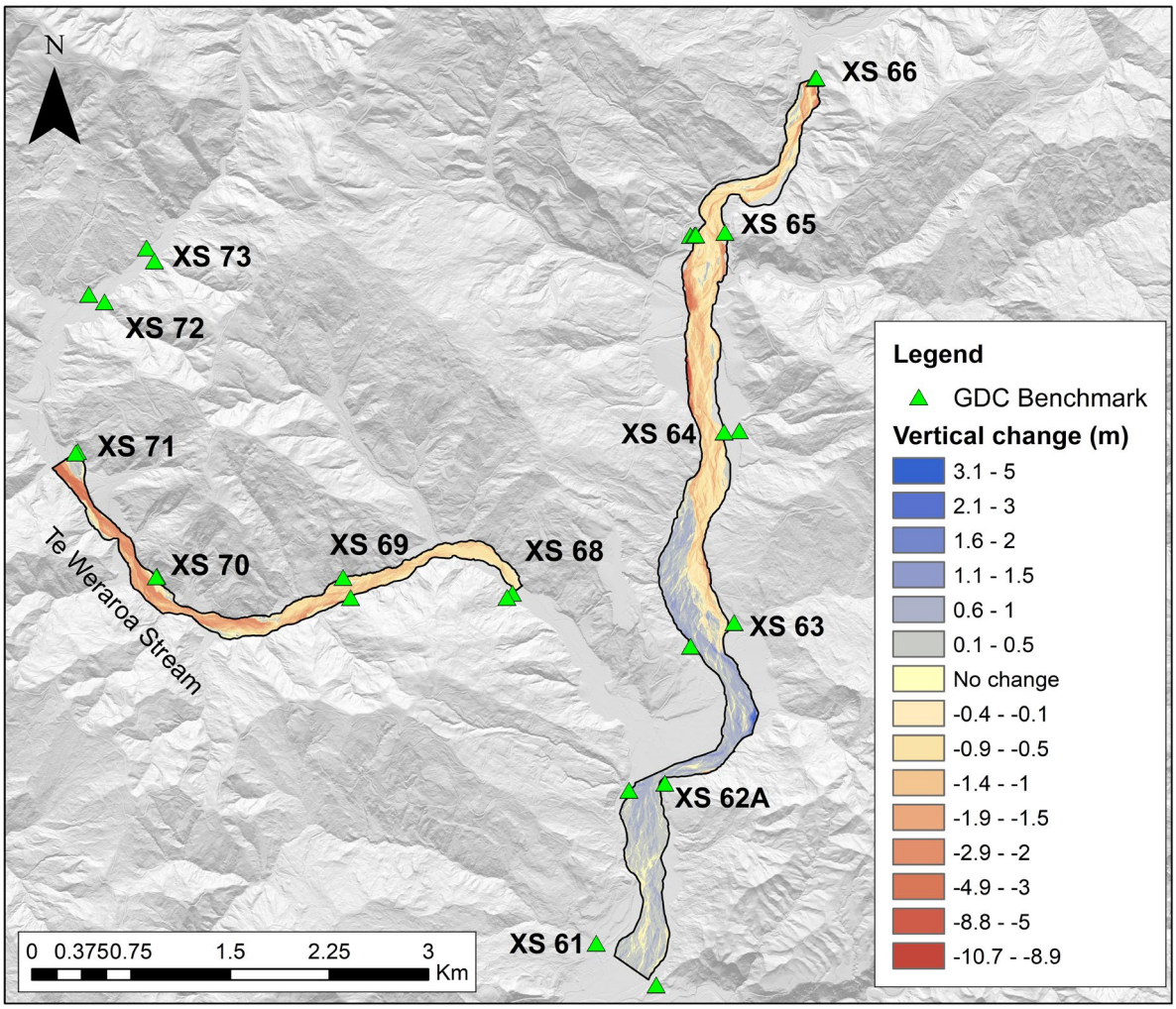

Figure 6.5 LiDAR difference model for the upper Waipaoa used for comparison to Gisborne District Council (GDC) cross-section surveys. The GDC benchmarks and cross-section locations are shown.

Table 6.6 Volumes of bed material eroded (degradation) and deposited (aggradation) in each of the Gisborne District Council XS comparison reaches between 2005 and 2019 from LiDAR differencing. All volumes are quoted in cubic metres.

Reach	Degradation	Aggradation	Deg. +1 σ	Deg. -1 σ	Agg. +1 σ	Agg. -1 σ	Net Change
Waipaoa XS 61–66	-805,590	404,720	-716,640	-901,340	502,770	313,474	-400,870
Te Weraroa XS 68–71	-633,010	14,110	-582,060	-685,410	20,290	9380	-618,900

Table 6.7 Summary of Waipaoa volume calculations from Gisborne District Council cross-section data. Data used in the calculations are presented in Table A2.1.

Year	Change in Sediment Volumes					Sum XS Volume Change	Cumulative Volume Change
	XS 61–62	XS 62–63	XS 63–64	XS 64–65	XS 65–66		
2004/05	-154,070	-132,640	4920	-970	-15,850	-298,610	-298,610
2005/07	-6030	24,060	22,660	-11,710	5580	34,570	-264,040
2007/09	15,960	-3080	-29,510	-53,200	-61,980	-131,800	-395,840
2009/10	19,550	-4930	-12,440	-29,930	5170	-22,580	-418,420
2010/14	58,310	64,370	-19,810	-81,270	-53,040	-31,450	-449,860
2014/19	-520	4640	-12,850	-58,130	-90,580	-157,440	-607,310
			Sum of Volume Change 2005–2019			**-308,700**	**-22,050 m^3/yr**

Table 6.8 Summary of Te Weraroa volume calculations from Gisborne District Council cross-section data. Data used in the calculations are presented in Table A2.2.

Year	Change in Sediment Volumes			Sum XS Volume Change	Cumulative Volume Change
	XS 68–69	XS 69–70	XS 70–71		
2005–2007	-5760	-26,690	-84,030	-116,470	-116,470
2007–2014	-73,490	-115,270	-327,290	-516,050	-632,530
2014–2019	-51,110	-93,930	-243,880	-388,920	-1,021,450
		Sum of Volume Change 2005–2019		**-1,021,450 m^3**	**-72,960 m^3/yr**

LiDAR typically does not penetrate water well, so some LiDAR points in the wetted channel may describe the water surface but not the underlying river bed. The 2019 GDC cross-section is compared to a section extracted from the 2019 LiDAR DEM in Figure 6.6. The plot shows the differences between the two survey techniques. The LiDAR data appears to have captured the river bed in the deeper parts of the channel sufficiently; however, the benchmarks are not well-aligned vertically (about +0.3 m out), so care will be needed to compare the two data sources. The two surveys were carried out on different dates, so sediment transport between the two surveys could also account for some of the differences.

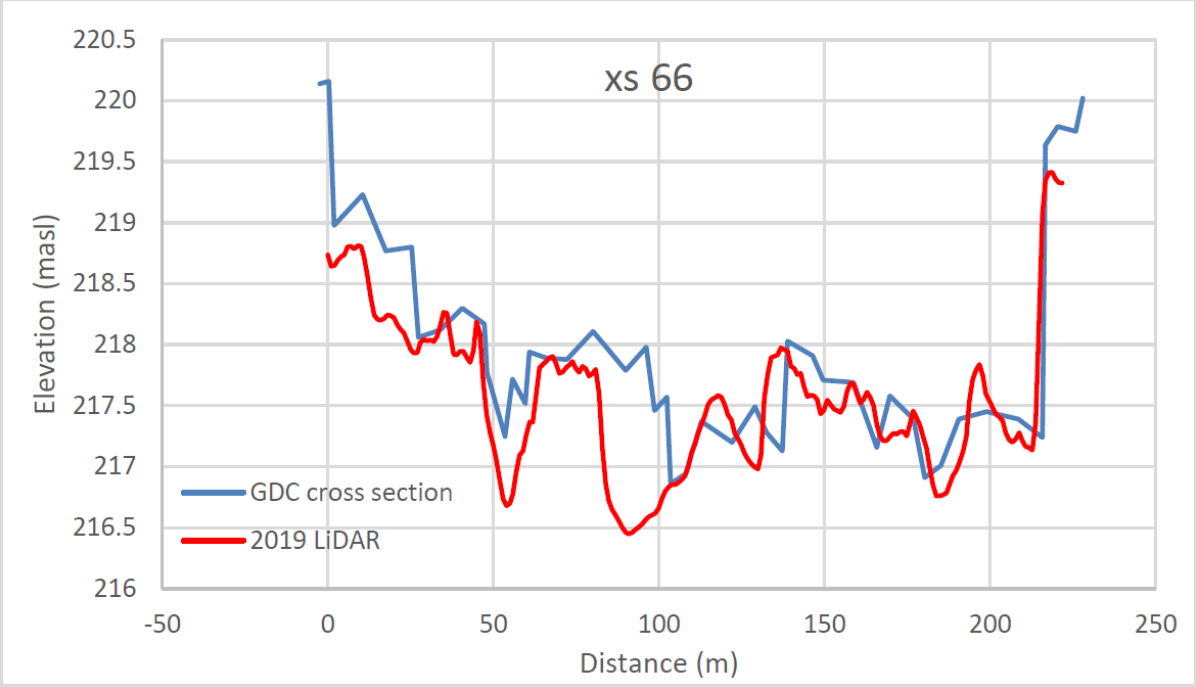

Figure 6.6 Cross-section profile plots for XS 66 in the upper Waipaoa reach derived from 2019 Gisborne District Council cross-section data and the 2019 LiDAR DEM.

7.0 DISCUSSION

7.1 LiDAR Differencing

Elevation changes in the active channel of the Waipaoa and Te Weraroa rivers derived from differencing of LiDAR DEMs from 2005 and 2019 show that there is now a dominant trend of channel incision in these reaches. The volumes of material eroded or stored in each of the study reaches were used to construct a crude sediment budget for the study area by calculating the volumes of sediment supplied to each reach, along with the volumes stored or eroded from each, using a mass balance approach. The sediment volumes and sediment budget are summarised in Figure 7.1. The sediment budget indicates that ~1,443,000 m^3 or ~103,000 m^3/yr was delivered to reaches downstream of the study area. Using a bulk density of 1.82 t/m^3 for Waipaoa riverbed material (Gomez et al. 2009), this is about 187,000 t/yr. This value is higher than Gomez et al.'s (2009) modelled estimate of long-term annual bedload discharge at Kanakanaia of 91.4 ± 53.5 Kt/yr but similar to the estimate of bedload as 1% of the 15 Mt/yr suspended sediment yield (150,000 t/yr) (Gomez et al. 2001). The volumes do not take into account sediment supplied by lateral sources, such as bank erosion and streamside landslides (Table 6.3), which could be significant in some reaches (Gomez et al. 2001; De Rose and Basher 2011; this study). Figure 7.2 summarises cumulative sediment deficit in relation to summed sediment gains and losses along the Waipaoa and Te Weraroa study reaches. The predominance of sediment losses in the upper Waipaoa, Te Weraroa and downstream of the gorge are apparent, as is the build-up of sediment upstream of the gorge and transfer of sediment through the gorge. The differences in the cumulative sediment deficit along the study reach – 1.35 Mm^3 using the total gains and losses for each 150 m segment (Figure 7.2) versus 1.33 Mm^3 for the Waipaoa main stem (Table 6.2) – can be explained by the exclusion of lateral sediment sources such as erosion of alluvial fans and bank erosion from the volumes in Figure 7.2; however, these volumes are small in comparison to the volumes of sediment eroded from the active bed.

From 2005 to 2019, the dominant trend was for channel incision in the top 5 km of the upper Waipaoa River study reach down to near the confluence with Te Weraroa Stream (XS 62). Most tributary reaches covered by the LiDAR differencing also showed a net loss of sediment in their lower reaches, upstream of the Waipaoa mainstem, including many of the large alluvial fans such as at the mouths of the Matau, Matekonekone and Gully 117 streams. In contrast to previous work on Te Weraroa Stream (Gomez et al. 2003), the stream also showed a net loss of bed material for most of its length between 2005 and 2019. In the lower kilometre of Te Weraroa Stream, sediment deposition exceeded erosion, resulting in slight aggradation near the confluence with the Waipaoa River. However, volumes of material removed by incision were ten times greater than those deposited in the Te Weraroa channel over the study period (Table 6.2). Gomez et al. (2003) noted that 48% of sediment generated from gully erosion in the catchment from 1950 to 1988 was retained in channel storage in Te Weraroa Stream. Aggradation rates and the cumulative volume of sediment stored in the Te Weraroa channel were beginning to slow by 1996, after reaching a peak around 1990 (1986–1992); however, they note that there had been very little bed degradation by 1996. Cross-section analysis indicates that the initial signs of degradation in the Te Weraroa headwaters were seen in the 1990s, and the channel has continued to degrade since then (Peacock and Marden 2019). From 2005 to 2019, ~-812,900 m^3 of material was transferred from Te Weraroa Stream to the mainstem. This is equivalent to ~-58,000 m^3/yr or 107,000 t/yr (bulk density of 1.84 t/m^3). Gomez et al. (2003) suggested that it would take many decades for the gravel stored along the lower reaches of Te Weraroa Stream to be released from storage; however, it appears that the process of gravel removal is well underway (23 years later).

Aggradation is still occurring in the Waipaoa River reach immediately upstream of the gorge, downstream of the confluence of Te Weraroa Stream, at a rate of +25 mm/yr. However, this is less than a third of the average rate of aggradation for this reach over the period 1948–2005 (71.8 mm/yr from GDC MBL data). This reach is aggrading at a much slower rate than in the past. It is very efficient at transporting sediment, as ~90% of the material delivered to this reach from the Te Weraroa and upper Waipaoa reaches was transferred to the gorge reach below. This reach is constrained at the downstream end by the gorge. From 2005 to 2019, the reach above the gorge appears to have been very efficient at transporting material out to the gorge, but this may not reflect the long-term trend, as increased aggradation rates and growing active width in this reach suggest that the gorge has restricted the transfer of bed material (both the size and volume of sediment) over the longer timeframe (Gomez et al. 2001).

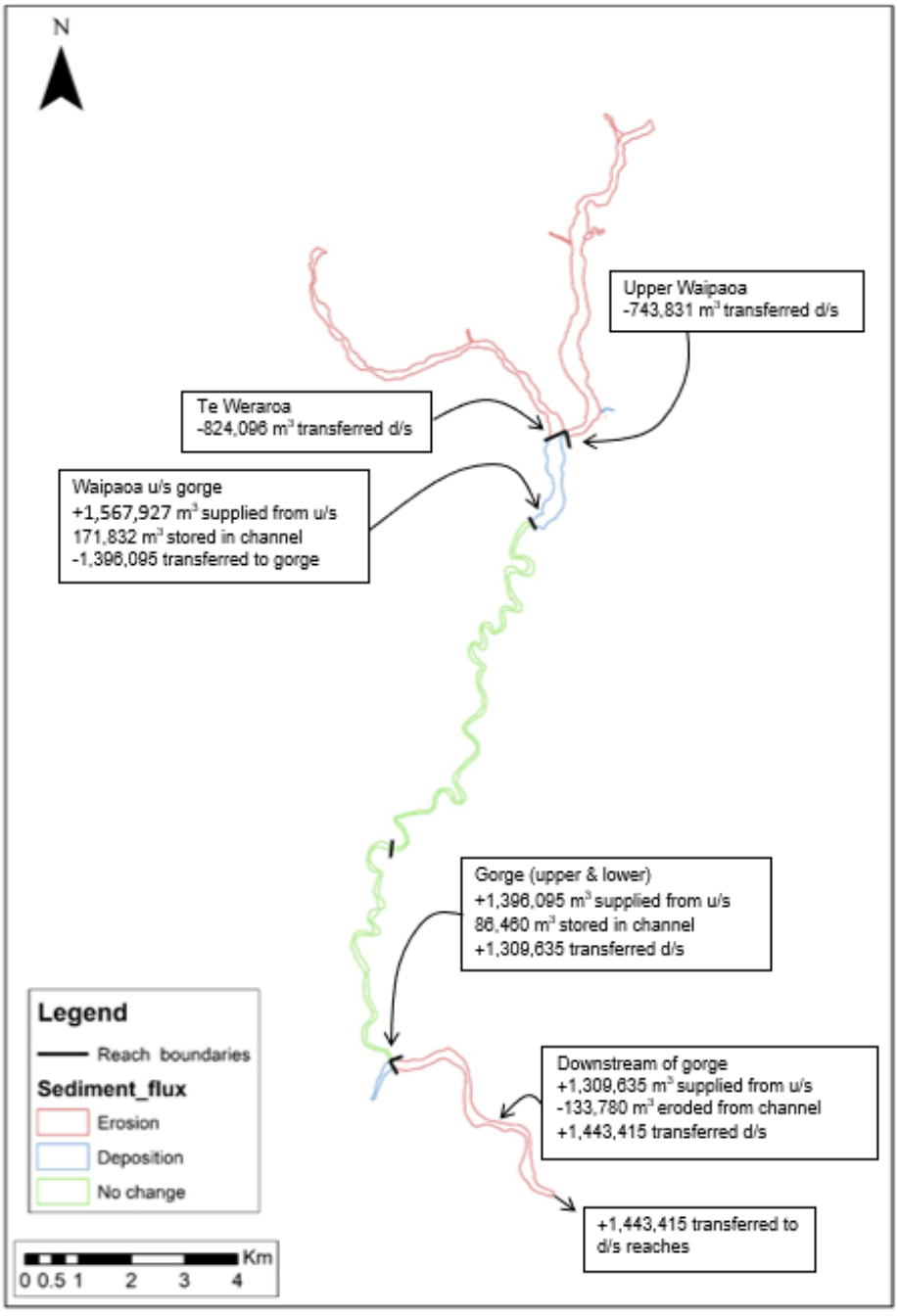

Figure 7.1 Conceptualised sediment budget for the study reaches based on the volumes of sediment eroded and deposited within each reach from the LiDAR differencing, 2005–2019.

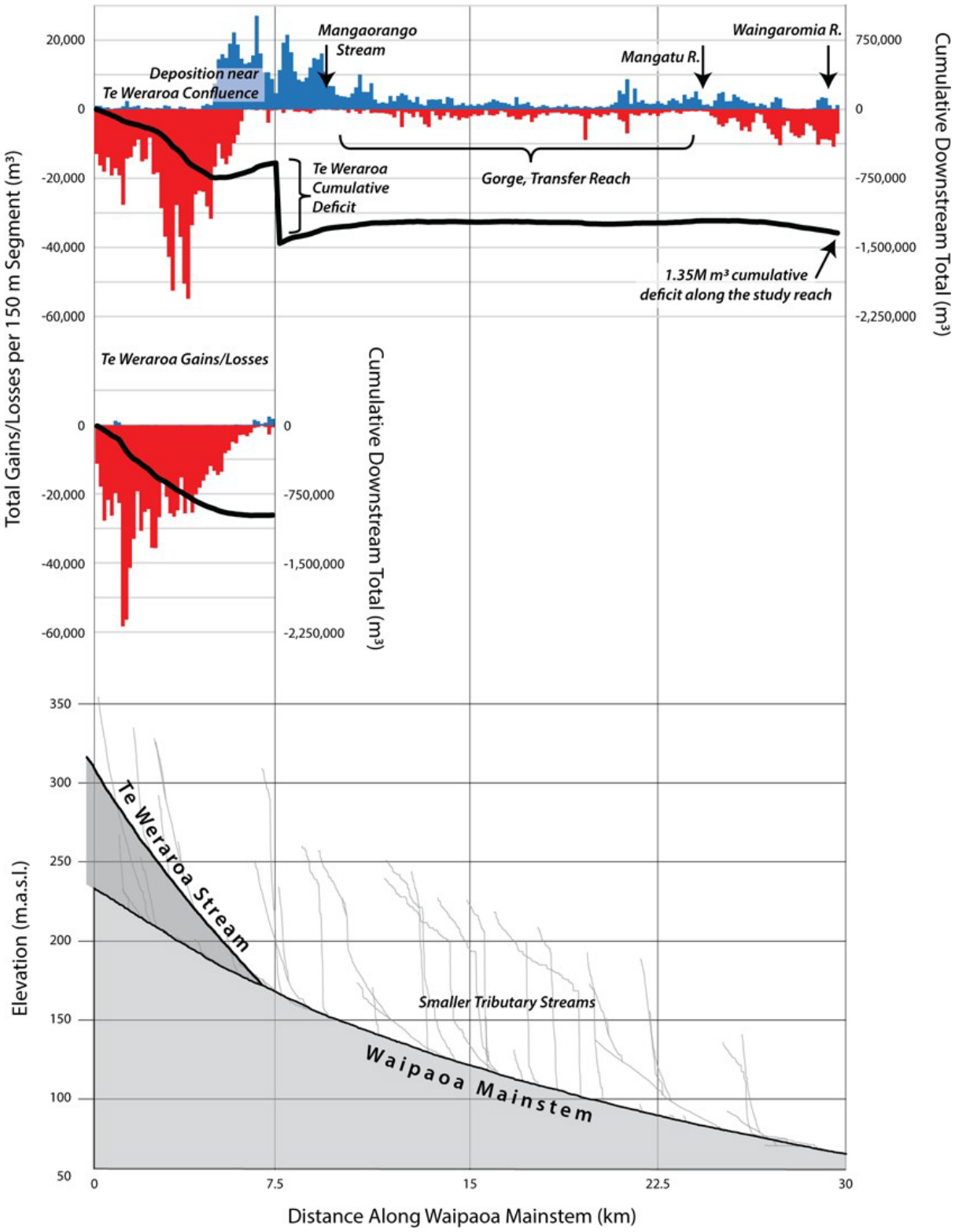

Figure 7.2 The cumulative sediment deficit from the LiDAR difference model shown in relation to the summed sediment gains and losses for each 150 m segment along the Waipaoa and Te Weraroa study reaches. Sediment gains are shown in blue and losses in red. Also shown are the longitudinal profiles of the Waipaoa River and Te Weraroa Stream and smaller tributaries.

The gorge reaches showed little change in mean bed level or volume of sediment. Volumes of material that accumulated in and eroded from the reach were roughly the same (Table 6.2), and 94% of the sediment volume supplied from upstream was transferred out. This is in agreement with the results of cross-section analysis, which showed that mean bed levels had not changed in this reach since 2005 and that the gorge was simply a sediment conduit, where

sediment is efficiently transported through (Peacock and Marden 2019). Peacock and Marden (2019) also noted that aggradation rates in this reach had slowed. Approximately 128,000 m^3 (equivalent to 16.800 t/yr) of material was supplied to this reach by streamside landslides and mass wasting processes on adjacent slopes directly coupled to the channel, which may account for some localised aggradation through the gorge reach. Cliff erosion is the dominant process, accounting for 69–88% of sediment delivered from channel-side processes within the gorge. The estimate of sediment derived from channel-side processes in this study is much less than the De Rose and Basher (2011) estimate of 97,600 t/y. This is likely because the mapping of channel-side processes in this project was not part of the initial objectives and was undertaken to give an indication of the suitability of LiDAR differencing to measure these volumes. Channel incision is also the dominant process in the reach immediately downstream of the gorge and at the confluence with the Mangatu River. The reach widens downstream from XS 51 (from 60 to 93 m; Table 5.1), and the channel morphology transitions back to a multi-thread braided channel configuration. Average aggradation rates (from GDC MBL data) in this reach (XS 48–51) for the years 2000–2003 and 2003–2009 were +24.8 mm/yr and +44.8 mm/yr, respectively.[1] From 2005 to 2019, mean bed level (from LiDAR differencing) in this reach declined by an average of -0.195 m (± 0.42), equivalent to -13.92 mm/yr, and indicates that channel incision has now extended downstream beyond the gorge.

An unknown quantity affecting this reach is the amount of bed material supplied from the Mangatu River. The very short reach of the Mangatu River covered by the 2005 LiDAR (0.8 km) means that we were not able to estimate sediment volumes supplied to this reach from the Mangatu River with any certainty, although the reach does appear to still be aggrading, suggesting that sediment supply exceeds the sediment transport capacity in that reach. The catchment area and erosion processes are similar for both the Mangatu and Waipaoa rivers at this point (Gomez and Livingston 2012); however, the suspended sediment yield for the Mangatu River (2.1 Mt/yr; Hicks et al. 2011) at Omapere (near the confluence with the Waipaoa River) is almost twice that of the Waipaoa River at Waipaoa Station (1.2 Mt/yr, Hicks et al. 2011), so it could be expected that an equal or greater sediment supply originates from the Mangatu River catchment, as from the upper Waipaoa River catchment. Peacock and Marden (2019) noted that MBL changes at XS 51 (at the confluence of Mangatu and Waipaoa) were generally more variable than at other cross-sections in the same reach, due to the influence of sediment supply from the Mangatu River.

The link between rainfall (storms), sediment supply (from erosion) and sediment transport in the upper Waipaoa catchment has been well documented (Marutani et al. 1999; Reid and Page 2003; Fuller and Marden 2011; Taylor et al. 2018). There were no extreme storm events (i.e. >20-year return interval) experienced in the study area over the study period, so the rates of sediment transfer through the channel network can be considered low, or close to ambient, annual rates over the long term (Taylor et al. 2018; Fuller et al. 2020). The maximum 24-hour rainfall over the study period was 161.8 mm in May 2011 (at Motu EWS near the top of the Waipaoa catchment), which has an annual return interval of 10 years (HIRDS: https://niwa.co.nz/information-services/hirds).

Tarndale and Mangatu gullies: LiDAR differencing of Tarndale and Mangatu gullies indicates that the two gully systems continue to enlarge and supply large volumes of material to the Te Weraroa and Mangatu rivers, although significant sediment storage is also apparent on the fans. Approximately -800,000 m^3 was delivered to Te Weraroa Stream from the

1 There was no 2005 or 2019 cross-section data available for XS 48–51. For the period 2009–2017, cross-section data was only available for XS 50 and 51, where the average rate of MBL change was +4.9 mm/yr.

Tarndale Gully complex, equivalent to ~105,000 t/yr delivered to Te Weraroa Stream. Over the same timeframe, a minimum of ~1,167,000 m^3 was delivered to the Mangatu River by the Mangatu Gully complex, equivalent to 153,000 t/yr delivered to Mangatu River.

Fuller et al. (2020) completed DEM differencing for the Tarndale and Mangatu gully complexes over the same time period as this study (2005–2019) and quantified volumes of sediment erosion and deposition from the two gullies as they co-evolved. Fuller et al. (2020) utilised the 2005 GDC LiDAR as a baseline and constructed a 2019 DEM using structure from motion stereo photogrammetry (SFM). The results from the LiDAR differencing in this study are in general agreement to the results obtained using SFM by Fuller et al. (2020), and the volume changes are generally within their error limits. The differences in volumes of sediment eroded and deposited between the two studies can be accounted for by differences in the area over which the calculations were performed. Fuller et al. (2020) excluded vegetated areas (in either 2005 or 2019) from their volume calculations; however, they were included in this study. The reader is referred to Fuller et al. (2020) for a more thorough discussion of the evolution of Tarndale and Mangatu gullies over the study period. A more thorough analysis of the differences between the two techniques is beyond the scope of this report. However, it is clear that the 2019 LiDAR DEM was able to pick up elevation changes in vegetated areas that were excluded from Fuller et al.'s (2020) 2019 SFM DEM. Examples include movement (surface lowering in the source area and raising in the lower portions) on deep-seated landslides in catchments A and B of Tarndale Gully and on the southern edge (true left) of Mangatu Gully (see Figure 6.3c).

7.2 River Response and Recovery

Understanding the pattern and rate of geomorphic response of a catchment to disturbance is important for predicting downstream impacts and consequent risks to society (Tunnicliffe et al. 2018). The headwater reaches of the Waipaoa River responded rapidly to increased sediment supply from hillslope destabilisation in the early 20th century by aggrading up to 10–12 m by the 1960s (Gomez et al. 2003; Peacock and Marden 2019). LiDAR differencing of the upper Waipaoa River confirms that channel degradation is now the dominant process in these reaches, and incision has progressed downstream at least as far as the confluence with the Waingaromia River. The channel incision is proceeding from the headwater reaches in the downstream direction, as the sediment supply has been successfully reduced in headwater catchments by reforestation (Gomez et al. 2003). This indicates that the river is responding to the decrease in sediment supply brought about by reforestation of headwater catchments and stabilisation of many of the gullies. A possible contributing factor is the lack of extreme storm events since Cyclone Bola in 1988, which mobilise and deliver sediment from hillslope erosion to the channel network.

The headwater reaches of the adjacent Waiapu River catchment are also starting to show signs of incision as the system adjusts to a reduced rate of sediment supply from hillslope erosion following reforestation (Tunnicliffe et al. 2018). Rapid aggradation of river channels of the adjacent Waiapu River catchment occurred in response to large inputs of hillslope material generated during Cyclone Bola in 1988 (Tunnicliffe et al. 2018). The Waiapu catchment is underlain by the same highly erodible geological units as the Waipaoa, but there is a larger proportion of the catchment affected by shear zones associated with the East Coast Allocthon and sediment yields are even higher than in the Waipaoa River (35 Mt/yr for the Waiapu compared to 15 Mt/yr for the Waipaoa; Hicks et al. 2000). Gully erosion is the dominant sediment source in the Waiapu catchment, where it accounts for 49% of the annual suspended sediment yield (Marden et al. 2008). Similar to the upper Waipaoa reaches, channel incision

was initiated in the headwater channels of the Waiapu River and has propagated downstream (Tunnicliffe et al. 2018). Page et al. (2007) suggest that the relative deficit of upstream sediment supply resulted in the evacuation of sediment stored in headwater reaches and possibly reflects the steep river profile and extensive bedrock control in these headwater streams (Tunnicliffe et al. 2018).

There is anecdotal evidence to suggest that as the Waipaoa River degrades the bed material in these reaches is becoming coarser (D Peacock pers. comm.; Figure 7.3): selective transport of the finer material leaves a lag of coarse material and armours the bed (Tunnicliffe et al. 2018). This may slow the rate of incision with time as a greater proportion of the bed becomes protected by the coarse armour layer. A similar process of surface bed material coarsening has been observed in the Waiapu River, as it cuts down in the headwater reaches (Tunnicliffe et al. 2018).

Figure 7.3 Waipaoa River channel at XS 65, taken in February 2010 by Dave Peacock, showing signs of degradation (cutting into the right bank and stabilisation of bar by vegetation) and exposure of coarse bed material. In 1996, the bed material D_{50} at this location was 4.32 mm sub-surface, 19.7 mm surface (Rosser 1997). By 2010, the surface particle size appears to be much coarser.

The transition from aggradation to degradation in the upper Waipaoa River indicates that the main sediment source is now likely to be from within the active alluvial plain, including the river beds and lateral sediment stores, such as floodplains, terraces and alluvial fans, rather than from mass movement and gully erosion in the headwater catchments. Sediment supply to downstream reaches will probably remain high as the river starts to cut down through the stored valley bottom material, as large volumes of mostly fine sediment are stored in the channel and are available for transport. There are also large volumes of fine sediment stored in alluvial fans adjacent to and encroaching upon the active channel. From 2005 to 2019, nearly -200,000 m^3 of sediment was eroded from alluvial fans in the upper Waipaoa reach alone (Figure 6.3).

The response of the Waipaoa River to disturbance (deforestation) in the headwaters was rapid (Gomez et al. 2001, 2007; Page et al. 2007; Peacock and Marden 2019), and the river's response to a decline in sediment supply appears to be equally as rapid. Large storm events (e.g. in 1938, 1948, 1988) that mobilised sediment in the upper Waipaoa have also impacted the rate at which sediment was supplied to the channel network in the historic period, resulting in a highly variable sediment yield. This study provides a snapshot in time of the longer-term response of the Waipaoa River system to multiple disturbances. Rapid aggradation in the headwater reaches (253 mm/yr from 1948 to 1965 at XS 66, GDC MBL data) in response to increased sediment supplied from accelerated erosion continued until about 1960 and, by the 1970s, most of the upper catchment had been re-forested, effectively reducing the rate that sediment was supplied to the channels from hillslope erosion (Gomez et al. 2003). The volume of bed material stored in the river channels in the upper Waipaoa catchment, above the gorge, peaked around 1992–1996 following Cyclone Bola in 1988 (Figure 7.4), and the rate of aggradation and sediment storage has slowed since this time (Peacock and Marden 2019). The initial stages of degradation became apparent in the early 1990s in the headwater reaches of the Waipaoa River; however, most of these reaches continued to aggrade, albeit at a slower rate. Twenty-five to thirty years later, incision is the dominant trend in the headwater reaches. Reforestation of the headwater catchments has reduced sediment supply to the channel network; however, the lack of extreme storm events since Cyclone Bola, and the exhaustion of sediment generated by this extreme storm, may also have contributed to the decline in sediment yield over this period.

Riverbed degradation appears to have progressed downstream at least as far as the Waingaromia River, at the downstream end of the study area. Differencing of the 2005 and 2019 LiDAR for the remainder of the Waipaoa River channel downstream of the Waingaromia River confluence will determine how far downstream the channel incision persists and verify contemporary rates of sedimentation on the bed and banks through the Waipaoa River Flood Control Scheme, which may help to determine further capacity losses in the scheme.

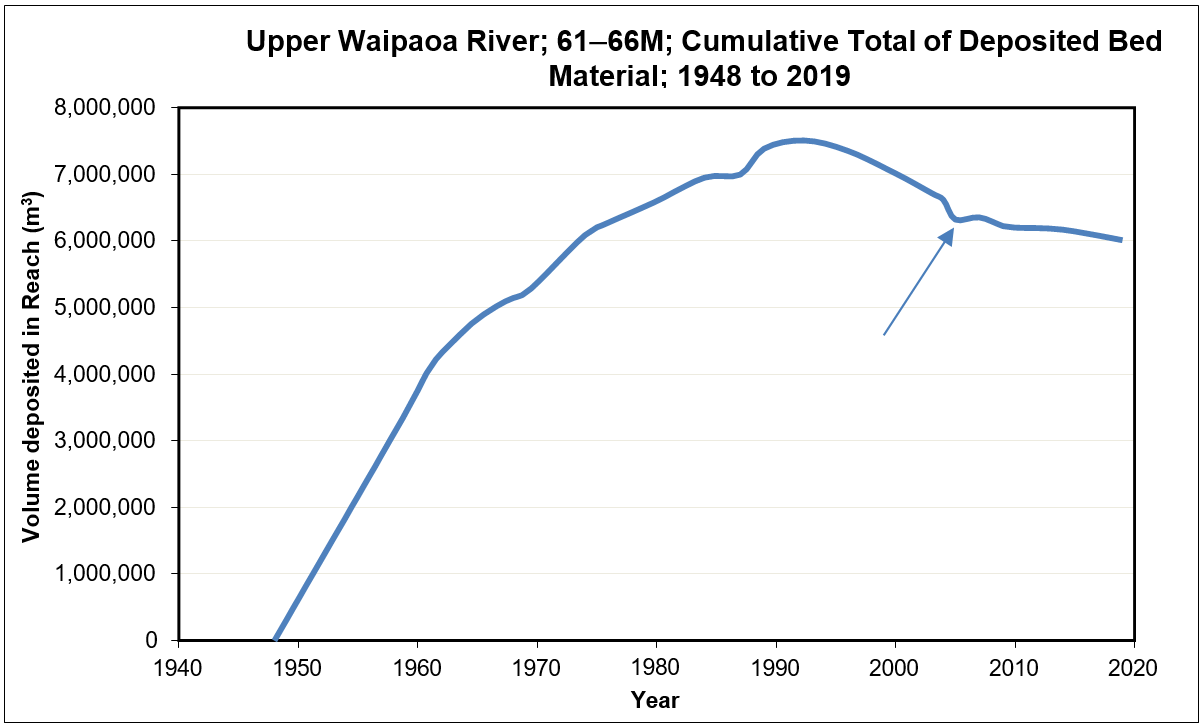

Figure 7.4 Cumulative total of bed material deposited between XS 61 and 66 over the period 1948–2019 (reproduced from Peacock and Marden [2019]). The arrow shows the beginning of the time period in this study. Cross-section surveys on the Waipaoa River began in 1948.

7.3 Comparison of LiDAR Differencing to XS Analysis

Bedload transport rates estimated using cross-section analysis are typically known to be under-estimated due to the compensating effects of erosion and deposition between cross-section surveys (Fuller et al. 2003; Tunnicliffe et al. 2018) and the tendency for cross-section surveys to 'miss' sediment that passes through a river section without causing erosion or deposition. The accuracy of cross-section surveys to estimate bedload transport depends on the spacing of cross-sections in relation to channel geometry and sediment sources, as well as the frequency of survey.

Comparison of sediment volume changes estimated using LiDAR differencing and traditional cross-section surveys yielded results of the same or similar magnitudes, although the magnitude of the differences was not consistent between the study reaches. When volume changes based on cross-section analysis were compared to the results from LiDAR differencing, changes in net sediment storage volumes were under-estimated in the Waipaoa River reach (XS 61–66) by about 23%, while cross-section analysis over-estimated sediment volume changes in the Te Weraroa reach (XS 68–71) by about 40%.

The application of LiDAR differencing is probably a more accurate technique to estimate sediment storage volume changes, as estimates of bed-level change are spatially continuous and are estimated for each 1 x 1 m pixel over the whole active channel area. Cross-section analysis, by contrast, is based on mean bed-level changes and cross-sectional areas extrapolated between cross-sections, which are on average 1.6 km apart. In Te Weraroa Stream, active channel width was much more variable than in the Waipaoa reach, and the average cross-sectional area did not reflect changes in the intervening narrower reaches; hence, sediment volume changes were over-estimated. Conversely, in the Waipaoa River, wider channel reaches between the XS benchmarks were not taken into account, resulting in sediment storage being under-estimated using the cross-section technique.

LiDAR differencing provides precise quantification of the net change in sediment storage in the study reaches between 2005 and 2019, but these volumes do not take into account inter-annual fluctuations in sediment storage during that timeframe. In particular, LiDAR differencing does not reveal the increase in the rate of aggradation in the upper Waipaoa reach between 2005 and 2007 that was detected in the cross-section analysis (Peacock and Marden 2019). LiDAR typically does not penetrate water well, so some LiDAR points in wetted channels describe the water surface but not the underlying river bed. The implication is that sediment volumes derived from LiDAR differencing represent a minimum estimate of sediment transfer (Fuller et al. 2003), and peaks in sediment storage or aggradation/degradation rates may be missed if they occur within the study period.

Sediment storage volumes estimated by LiDAR differencing are undoubtedly more accurate compared to cross-section analysis (Fuller et al. 2003), but aerial LiDAR surveys are expensive, hence there are trade-offs between survey accuracy and precision and the number or area of surveys that can be completed. With recent advances in drone-based collection of topographic data (Gallay 2013), high-resolution DEMs can now be produced using SFM from aerial photography (Fuller et al. 2020), and LiDAR data can be collected directly by drone (unmanned aerial vehicle). Channel reaches of concern could be targeted using drone surveys to produce DEMs of whole channel reaches on a more regular basis (e.g. yearly) than is practical for collection of regional LiDAR surveys. Alternatively, a hybrid approach could be employed where the change in mean bed level could be estimated at each cross-section using traditional surveying techniques and the active channel area between cross-sections could be measured directly from the 2019 LiDAR survey, replacing the averaged cross-sectional areas.

Differencing of DEMs constructed from LiDAR allows reliable estimates of the uncertainty of the sediment volume changes to be calculated (by determining the standard error of the difference model), as well as showing the spatial patterns of erosion and deposition within a reach, a feature that cross-section-based approaches may fail to include (Fuller et al. 2003). Nevertheless, the length of record and regularity (both in time and space) of cross-section surveys in the Waipaoa (and Waiapu) River means that the response of the rivers to both an increase and decrease in sediment supply over the last 58 years is very well documented (Gomez et al. 2003, 2006, 2009; Tunnicliffe et al. 2018).

8.0 CONCLUSIONS

- Elevation changes in the active channel of the Waipaoa and Te Weraroa rivers derived from differencing of LiDAR DEMs from 2005 and 2019 show that there is now a dominant trend of channel incision in these reaches. The channel incision was initiated in the headwater reaches and proceeded in the downstream direction as far as the confluence with the Waingaromia River (near Whatatutu, XS 48).
- Sediment storage changes estimated using LiDAR differencing show that from 2005 to 2019, ~2,291,000 m^3 of riverbed material was removed from the study reach and ~859,000 m^3 was deposited. This gives an overall net loss of sediment from the study reach of ~-1,432,200 m^3, or an average of ~-102,000 m^3/yr. Using a dry bulk density of Waipaoa riverbed material of ~1.82 t/ m^3 (Gomez et al. 2009), this equates to ~185,640 t/yr of bedload transfer.
- A similar pattern of channel response has been documented in the adjacent Waiapu catchment by Tunnicliffe et al. (2018). Incision began in the headwater reaches in 2007 and has progressed downstream as the sediment supply from upstream has declined.
- Mapping of sediment sources adjacent to and along the active channel using LiDAR differencing indicate that ~180,000 m^3 of material was supplied to the channel from bank erosion and streamside landslides (not included in the active channel difference volumes) and ~263,000 m^3 of the sediment loss within the 2005–2019 active channel was due to bank erosion or streamside landslides. Erosion of alluvial fans in the upper Waipaoa reach was significant, where ~-200,000 m^3 of sediment was released from the alluvial fans of Matau, Matakonoknoe and Gully 117.
- With the exception of the gorge reach, which acts as a sediment conduit, the overall trend is now degradation in most upper Waipaoa River reaches. This evidence is consistent with the notion that the river is starting to respond to the reduction in sediment supply due to erosion control efforts (Mangatu forest) in the headwater catchments and that reforestation has been successful at reducing the sediment supply to the Waipaoa River.
- The implication of this transition from aggradation to degradation in the headwater reaches is that the dominant sediment supply source may now switch to being the sediment in valley bottom stores such as floodplains, terraces and fans, as well as the active riverbed. In addition, sediment is still being supplied from badass gullies that are too big to be controlled by reforestation.
- Differencing of airborne LiDAR is very effective for developing a river sediment budget along several tens of river kilometres on a time-scale that could range from inter-event to inter-decadal, as in the present study. LiDAR and cross-section analyses produced similar estimates of sediment storage volume changes; however, cross-section surveys inherently involve significant spatial averaging (>1 km), leading to reduced accuracy.
- LiDAR differencing provides relatively precise quantification of the net change in sediment storage in the study reaches between 2005 and 2019, as well as the uncertainties associated with them, but the temporal resolution is very poor (absent) owing to the rarity of LiDAR surveys. The cross-section records reveal important pulses and dynamic behaviour that is clearly absent from the LiDAR record.

- Sediment storage volumes estimated by LiDAR differencing are undoubtedly more accurate compared to cross-section analysis but are very expensive; hence, there are trade-offs between survey accuracy and precision and the temporal resolution. Channel reaches of concern could be targeted using SFM or LiDAR drone surveys to produce DEMs of whole channel reaches on a more regular basis (e.g. yearly) than is practical for regional LiDAR surveys.
- Historic volume estimates using cross-sections could be improved by using the active channel area for reaches in between cross-sections from the 2019 LiDAR rather than averaging widths.

9.0 RECOMMENDATIONS

- No fieldwork was undertaken as part of this study. It would be beneficial to undertake fieldwork in the study area to identify morphological evidence to verify the channel degradation identified in the LiDAR differencing.
- Differencing of the 2005 and 2019 LiDAR for the remainder of the Waipaoa River channel will show the downstream extent of channel incision and help to quantify rates of sedimentation on the bed and banks of the Waipaoa River through the Waipaoa River Flood Control Scheme, which could be used to determine further capacity losses.
- Further understanding of sediment sources along the study reach could be gained by linking sediment supply to processes (fans, landslides, etc.) on a geomorphic map. More detailed mapping of sediment sources on the adjacent hillslopes and determination of the errors associated with the difference model on these slopes is recommended to better quantify these sediment sources.

10.0 ACKNOWLEDGEMENTS

Funding for this study was provided by Envirolink. Gisborne District Council provided the LiDAR data, aerial photography and cross-section data for the Waipaoa and Te Weraroa rivers. Dave Heron of GNS Science assisted by building DEMs of the study area and ensuring that the correct vertical and horizontal datums were applied. Dave Peacock provided mean bed-level and sediment volume data for the upper Waipaoa River. The authors thank Jon Tunnicliffe of Auckland University and Andrea Wolter (GNS Science) for reviewing the report. Jon Tunnicliffe also kindly provided Figure 7.2.

11.0 REFERENCES

AAM Hatch. 2006. Digital data documentation. Gisborne District Council, airborne laser survey of the Waipaoa River floodplain. Volume 10031A01NOB. [Napier] (NZ): AAM Hatch. 18 p.

Aerial Surveys Ltd. 2020. Metadata, Gisborne District Council, East Coast – Tairawhiti 2018/19 LiDAR Survey. Aerial Surveys Project №: FPFA1228. [Auckland] (NZ): Aerial Surveys Ltd. 6 p.

Allsop F. 1973. The story of Mangatu: the forest which healed the land. Wellington (NZ): Government Printer. 99 p. (New Zealand Forest Service information series; 62).

Beavan J, Motagh M, Fielding EJ, Donnelly N, Collett D. 2012. Fault slip models of the 2010–2011 Canterbury, New Zealand, earthquakes from geodetic data and observations of postseismic ground deformation. *New Zealand Journal of Geology and Geophysics*. 55(3):207–221. doi:10.1080/00288306.2012.697472.

Bernard TG, Lague D, Steer P. 2021. Beyond 2D landslide inventories and their rollover: synoptic 3D inventories and volume from repeat lidar data. *Earth Surface Dynamics*. 9(4):1013–1044. doi:10.5194/esurf-9-1013-2021.

Black RD. 1980. Upper Cretaceous and Tertiary geology of Mangatu State Forest, Raukumara Peninsula, New Zealand. *New Zealand Journal of Geology and Geophysics*. 23(3):293–312. doi:10.1080/00288306.1980.10424141.

Brierley GJ, Fryirs K. 2000. River styles, a geomorphic approach to catchment characterization: implications for river rehabilitation in Bega catchment, New South Wales, Australia. *Environmental Management*. 25(6):661–679. doi:10.1007/s002670010052.

Bull JM, Miller H, Gravley DM, Costello D, Hikuroa DCH, Dix JK. 2010. Assessing debris flows using LIDAR differencing: 18 May 2005 Matata event, New Zealand. *Geomorphology*. 124(1–2):75–84. doi:10.1016/j.geomorph.2010.08.011.

Chorley RJ. 1962. Geomorphology and general systems theory. Washington (DC): US Government Printing Office. 10 p. Geological Survey Professional Paper 500-B.

Clark KJ, Nissen EK, Howarth JD, Hamling IJ, Mountjoy JJ, Ries WF, Jones K, Goldstien S, Cochran UA, Villamor P, et al. 2017. Highly variable coastal deformation in the 2016 MW7.8 Kaikōura earthquake reflects rupture complexity along a transpressional plate boundary. *Earth and Planetary Science Letters*. 474:334–344. doi:10.1016/j.epsl.2017.06.048.

De Rose RC, Basher LR. 2011. Measurement of river bank and cliff erosion from sequential LIDAR and historical aerial photography. *Geomorphology*. 126(1–2):132–147. doi:10.1016/j.geomorph.2010.10.037.

De Rose RC, Gomez B, Marden M, Trustrum NA. 1998. Gully erosion in Mangatu Forest, New Zealand, estimated from digital elevation models. *Earth Surface Processes and Landforms*. 23(11):1045–1053.

Duffy B, Quigley M, Barrell DJA, Van Dissen R, Stahl T, Leprince S, McInnes C, Bilderback E. 2013. Fault kinematics and surface deformation across a releasing bend during the 2010 MW 7.1 Darfield, New Zealand, earthquake revealed by differential LiDAR and cadastral surveying. *GSA Bulletin*. 125(3–4):420–431. doi:10.1130/b30753.1.

Fryirs K, Brierley G. 2000. A geomorphic approach to the identification of river recovery potential. *Physical Geography*. 21(3):244–277. doi:10.1080/02723646.2000.10642708.

Fryirs K, Brierley G. 2012. Geomorphic analysis of river systems: an approach to reading the landscape. Hoboken (NJ): Blackwell Publishing. 345 p.

Fuller IC, Large ARG, Charlton ME, Heritage GL, Milan DJ. 2003. Reach-scale sediment transfers: an evaluation of two morphological budgeting approaches. *Earth Surface Processes and Landforms*. 28(8):889–903. doi:10.1002/esp.1011.

Fuller IC, Marden M. 2010. Rapid channel response to variability in sediment supply: cutting and filling of the Tarndale Fan, Waipaoa catchment, New Zealand. *Marine Geology*. 270(1–4):45–54. doi:10.1016/j.margeo.2009.10.004.

Fuller IC, Marden M. 2011. Slope–channel coupling in steepland terrain: a field-based conceptual model from the Tarndale gully and fan, Waipaoa catchment, New Zealand. *Geomorphology*. 128(3–4):105–115. doi:10.1016/j.geomorph.2010.12.018.

Fuller IC, Strohmaier F, McColl ST, Tunnicliffe J, Marden M. 2020. Badass gully morphodynamics and sediment generation in Waipaoa Catchment, New Zealand. *Earth Surface Processes and Landforms*. 45(15):3917–3930. doi:10.1002/esp.5010.

Gage M, Black RD. 1979. Slope-stability and geological investigations at Mangatu State Forest. Wellington (NZ): New Zealand Forest Service. 37 p. (Technical Paper; 66).

Gallay M. 2013. Direct acquisition of data: airborne laser scanning. In: Cook S, Clarke L, Nield J, editors. *Geomorphological techniques.* London (GB): British Society for Geomorphology; [accessed 2021 Dec]. https://www.geomorphology.org.uk/sites/default/files/chapters/2.1.4_LiDAR.pdf

Gisborne District Council. 2020. Gisborne (NZ): Gisborne District Council. Waipaoa flood control: flood control climate change resilience project; [accessed 2021 Oct 21] https://www.gdc.govt.nz/council/major-projects/waipaoa-river-flood-control-scheme.

Gomez B. 1991. Bedload transport. *Earth-Science Reviews*. 31(2):89–132. doi:10.1016/0012-8252(91)90017-A.

Gomez B, Banbury K, Marden M, Trustrum NA, Peacock DH, Hoskin PJ. 2003. Gully erosion and sediment production: Te Weraroa Stream, New Zealand. *Water Resources Research*. 39(7):1187. doi:10.1029/2002WR001342.

Gomez B, Coleman SE, Sy VWK, Peacock DH, Kent M. 2007. Channel change, bankfull and effective discharges on a vertically accreting, meandering, gravel-bed river. *Earth Surface Processes and Landforms*. 32(5):770–785. doi:10.1002/esp.1424.

Gomez B, Cui Y, Kettner AJ, Peacock DH, Syvitski JPM. 2009. Simulating changes to the sediment transport regime of the Waipaoa River, New Zealand, driven by climate change in the twenty-first century. *Global and Planetary Change*. 67(3–4):153–166. doi:10.1016/j.gloplacha.2009.02.002.

Gomez B, Eden DN, Hicks DM, Trustrum NA, Peacock DH, Wilmshurst J. 1999. Contribution of floodplain sequestration to the sediment budget of the Waipaoa River, New Zealand. In: Marriott SB, editor. *Floodplains: interdisciplinary approaches*. London (GB): Geological Society of London. p. 69–88. (Geological Society special publication; 163).

Gomez B, Livingston DM. 2012. The river it goes right on: post-glacial landscape evolution in the upper Waipaoa River basin, eastern North Island, New Zealand. *Geomorphology*. 159–160:73–83. doi:10.1016/j.geomorph.2012.03.006.

Gomez B, Rosser BJ. 2018. Slip slidin' away: a post-glacial environmental history of the Waipaoa River basin. *Geomorphology*. 307:65–76. doi:10.1016/j.geomorph.2017.08.035.

Gomez B, Rosser BJ, Peacock DH, Hicks DM, Palmer JA. 2001. Downstream fining in a rapidly aggrading gravel bed river. *Water Resources Research*. 37(6):1813–1823. doi:10.1029/2001WR900007.

Griffiths GA. 1979. Recent sedimentation history of the Waimakariri River, New Zealand. *Journal of Hydrology (New Zealand)*. 18(1):6–28.

Herzig A, Dymond JR, Marden M. 2011. A gully-complex model for assessing gully stabilisation strategies. *Geomorphology*. 133(1–2):23–33. doi:10.1016/j.geomorph.2011.06.012.

Hicks DM, Gomez B, Trustrum NA. 2000. Erosion thresholds and suspended sediment yields, Waipaoa River Basin, New Zealand. *Water Resources Research*. 36(4):1129–1142. doi:10.1029/1999WR900340.

Hicks DM, Gomez B, Trustrum NA. 2004. Event suspended sediment characteristics and the generation of hyperpycnal plumes at river mouths: East Coast Continental Margin, North Island, New Zealand. *The Journal of Geology*. 112(4):471–485. doi:10.1086/421075.

Hicks DM, Shankar U, McKerchar AI, Basher L, Jessen M, Lynn I, Page M. 2011. Suspended sediment yields from New Zealand rivers. *Journal of Hydrology (New Zealand)*. 50(1):81–142.

Kasai M, Brierley GJ, Page MJ, Marutani T, Trustrum NA. 2005. Impacts of land use change on patterns of sediment flux in Weraamaia catchment, New Zealand. *CATENA*. 64(1):27–60. doi:10.1016/j.catena.2005.06.014.

Kasai M, Marutani T, Reid LM, Trustrum NA. 2001. Estimation of temporally averaged sediment delivery ratio using aggradational terraces in headwater catchments of the Waipaoa River, North Island, New Zealand. *Earth Surface Processes and Landforms*. 26(1):1–16. doi:10.1002/1096-9837(200101)26:1<1::AID-ESP146>3.0.CO;2-9.

Kuehl SA, Alexander CR, Blair NE, Harris CK, Marsaglia KM, Ogston AS, Orpin AR, Roering JJ, Bever AJ, Bilderback EL, et al. 2016. A source-to-sink perspective of the Waipaoa River margin. *Earth-Science Reviews*. 153:301–334. doi:10.1016/j.earscirev.2015.10.001.

Lane SN, Westaway RM, Murray Hicks D. 2003. Estimation of erosion and deposition volumes in a large, gravel-bed, braided river using synoptic remote sensing. *Earth Surface Processes and Landforms*. 28(3):249–271. doi:10.1002/esp.483.

Leenman A, Tunnicliffe J. 2018. Genesis of a major gully mass-wasting complex, and implications for valley filling, East Cape, New Zealand. *GSA Bulletin*. 130(7–8):1121–1130. doi:10.1130/b31849.1.

Marden M, Arnold G, Gomez B, Rowan D. 2005. Pre- and post-reforestation gully development in Mangatu Forest, East Coast, North Island, New Zealand. *River Research and Applications*. 21(7):757–771. doi:10.1002/rra.882.

Marden M, Arnold G, Seymour A, Hambling R. 2012. History and distribution of steepland gullies in response to land use change, East Coast Region, North Island, New Zealand. *Geomorphology*. 153–154:81–90. doi:10.1016/j.geomorph.2012.02.011.

Marden M, Betts H, Arnold G, Hambling R. 2008. Gully erosion and sediment load: Waipaoa, Waiapu and Uawa rivers, eastern North Island, New Zealand. In: Schmidt J, Cochrane T, Phillips C, Elliot S, Davies T, Basher L, editors. *Sediment dynamics in changing environments*. Wallingford (GB): International Association of Hydrological Sciences. p. 339–350. (IAHS publication; 325).

Marden M, Fuller IC, Herzig A, Betts HD. 2018. Badass gullies: fluvio-mass-movement gully complexes in New Zealand's East Coast region, and potential for remediation. *Geomorphology*. 307:12–23. doi:10.1016/j.geomorph.2017.11.012.

Marden M, Herzig A, Basher L. 2014. Erosion process contribution to sediment yield before and after the establishment of exotic forest: Waipaoa catchment, New Zealand. *Geomorphology*. 226:162–174. doi:10.1016/j.geomorph.2014.08.007.

Marutani T, Kasai M, Reid LM, Trustrum NA. 1999. Influence of storm-related sediment storage on the sediment delivery from tributary catchments in the upper Waipaoa River, New Zealand. *Earth Surface Processes and Landforms*. 24(10):881–896. doi:10.1002/(SICI)1096-9837(199909)24:10<881::AID-ESP17>3.0.CO;2-I.

Massey CI, Townsend DB, Rathje E, Allstadt KE, Lukovic B, Kaneko Y, Bradley B, Wartman J, Jibson RW, Petley DM, et al. 2018. Landslides triggered by the 14 November 2016 Mw 7.8 Kaikoura earthquake, New Zealand. *Bulletin of the Seismological Society of America*. 108(3B):1630–1648. doi:10.1785/0120170305.

Massey CI, Townsend DT, Lukovic B, Morgenstern R, Jones K, Rosser B, de Vilder S. 2020. Landslides triggered by the M_W7.8 14 November 2016 Kaikōura earthquake: an update. *Landslides*. 17(10):2401–2408. doi:10.1007/s10346-020-01439-x.

Mazengarb C, Francis DA, Moore PR. 1991. Geology of the Tauwhareparae area. Wellington (NZ): Department of Scientific and Industrial Research. 1 booklet. (Geological map of New Zealand 1:50 000; sheet Y16). Booklet accompanies the geological map.

Mazengarb C, Speden IG. 2000. Geology of the Raukumara area [map]. Lower Hutt (NZ): Institute of Geological & Nuclear Sciences Limited. 60 p. + 1 folded map., scale 1:250,000. (Institute of Geological & Nuclear Sciences 1:250,000 geological map; 6).

Moore PR, Mazengarb C. 1992. Geology and landforms of Raukumara Peninsula. In: Soons JM, Selby MJ, editors. *Landforms of New Zealand*. 2nd ed. Auckland (NZ): Longman Paul. p. 334–343.

Page M, Marden M, Kasai M, Gomez B, Peacock D, Betts H, Parkner T, Marutani T, Trustrum N. 2007. Changes in basin-scale sediment supply and transfer in a rapidly transformed New Zealand landscape. In: Habersack H, Piégay H, Rinaldi M, editors. *Gravel-bed rivers VI: from process understanding to river restoration*. Amsterdam (NL): Elsevier. p. 337–356. (Developments in earth surface processes;11).

Peacock DH, 1991. Waipaoa River Flood Control Scheme aggradation study. Gisborne (NZ): Gisborne District Council. Report No. EW2996.

Peacock DH, Marden M 2019. Mean bed level trends in the upper Waipaoa River channel and Te Weraroa Stream in response to land use change: 1948 to 2019. [Waikanae] (NZ): Peacock D H Ltd. 21 p.

Peacock DH, Philpott J. 2009. Waipaoa River Flood Control Scheme review. [Palmerston North] (NZ): Peacock D H Ltd and John Philpott and Associates Ltd. 27 p.

Procter J, Cronin SJ, Fuller IC, Lube G, Manville V. 2010. Quantifying the geomorphic impacts of a lake-breakout lahar, Mount Ruapehu, New Zealand. *Geology*. 38(1):67–70. doi:10.1130/g30129.1.

Procter JN, Cronin SJ, Zernack AV, Lube G, Stewart RB, Nemeth K, Keys H. 2014. Debris flow evolution and the activation of an explosive hydrothermal system; Te Maari, Tongariro, New Zealand. *Journal of Volcanology and Geothermal Research*. 286:303–316. doi:10.1016/j.jvolgeores.2014.07.006.

Reid LM, Page MJ. 2003. Magnitude and frequency of landsliding in a large New Zealand catchment. *Geomorphology*. 49(1–2):71–88. doi:10.1016/S0169-555X(02)00164-2.

Rosser BJ. 1997. Downstream fining in the Waipaoa River: an aggrading, gravel-bed river, East Coast, New Zealand. [MSc thesis]. Palmerston North (NZ): Massey University. 160 p.

Taylor RJ, Massey C, Fuller IC, Marden M, Archibald G, Ries W. 2018. Quantifying sediment connectivity in an actively eroding gully complex, Waipaoa catchment, New Zealand. *Geomorphology*. 307:24–37. doi:10.1016/j.geomorph.2017.10.007.

Thompson CS. 1987. The climate and weather of Hawke's Bay. 2nd ed. Wellington (NZ): New Zealand Meteorological Service. 46 p. (New Zealand Meteorological Service miscellaneous publication; 115(5)).

Trustrum NA, Gomez B, Page MJ, Reid LM, Hicks DM. 1999. Sediment production and output: the relative role of large magnitude events in steepland catchments. *Zeitschrift fur Geomorphologie*. Supplement 115:71–86.

Tunnicliffe J, Brierley G, Fuller IC, Leenman A, Marden M, Peacock D. 2018. Reaction and relaxation in a coarse-grained fluvial system following catchment-wide disturbance. *Geomorphology*. 307:50–64. doi:10.1016/j.geomorph.2017.11.006.

Wheaton JM, Brasington J, Darby SE, Sear DA. 2010. Accounting for uncertainty in DEMs from repeat topographic surveys: improved sediment budgets. *Earth Surface Processes and Landforms*. 35(2):136–156. doi:10.1002/esp.1886.

Williams RD. 2012. DEMs of difference. In: Cook S, Clarke L, Nield J, editors. *Geomorphological techniques.* London (GB): British Society for Geomorphology; [accessed 2021 Dec]. https://www.geomorphology.org.uk/sites/default/files/geom_tech_chapters/2.3.2_DEMsOfDifference.pdf

This page left intentionally blank.

APPENDICES

This page left intentionally blank.

APPENDIX 1 LIDAR DIFFERENCE MODELS FOR INDIVIDUAL STUDY REACHES

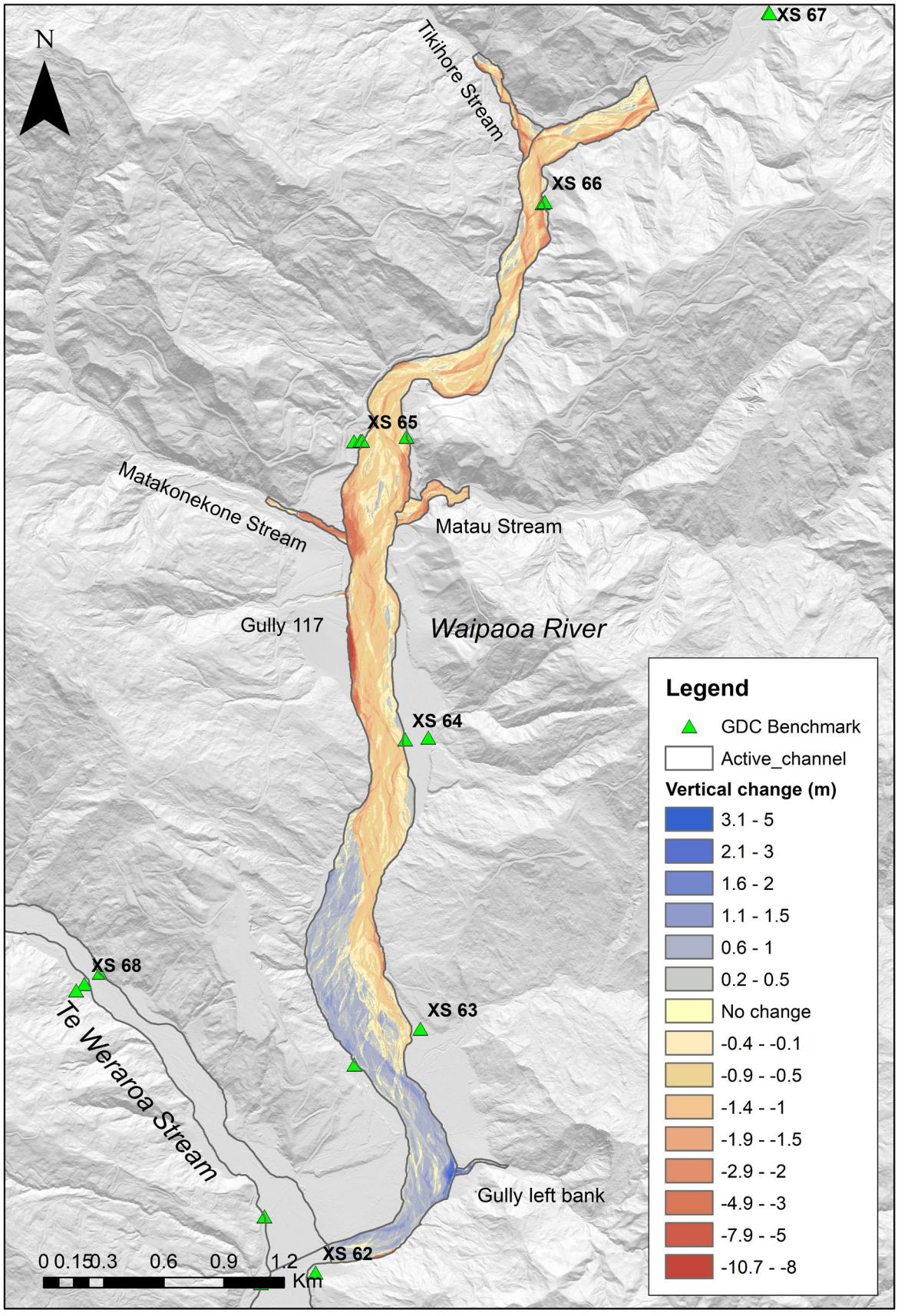

Figure A1.1 LiDAR difference model showing the vertical elevation change (in metres) for the upper Waipaoa reach.

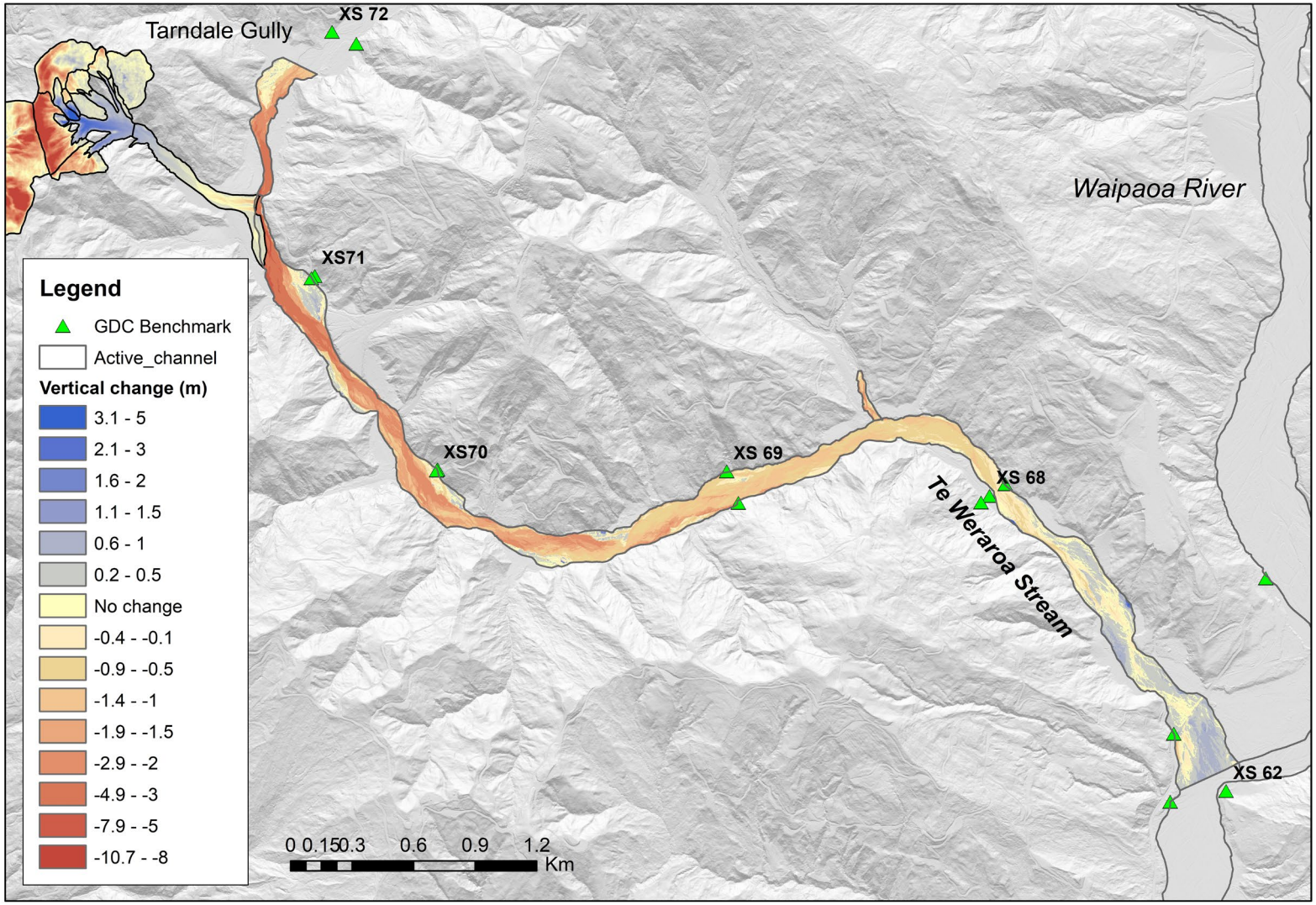

Figure A1.2 LiDAR digital elevation model of difference showing the vertical elevation change (in metres) for the Te Weraroa River reach. Note that the vertical change scale for Tarndale and Mangatu gullies is greater than for Te Weraroa but is just shown here for reference. See Figure 6.2 for more detail about elevation changes at Tarndale and Mangatu gullies.

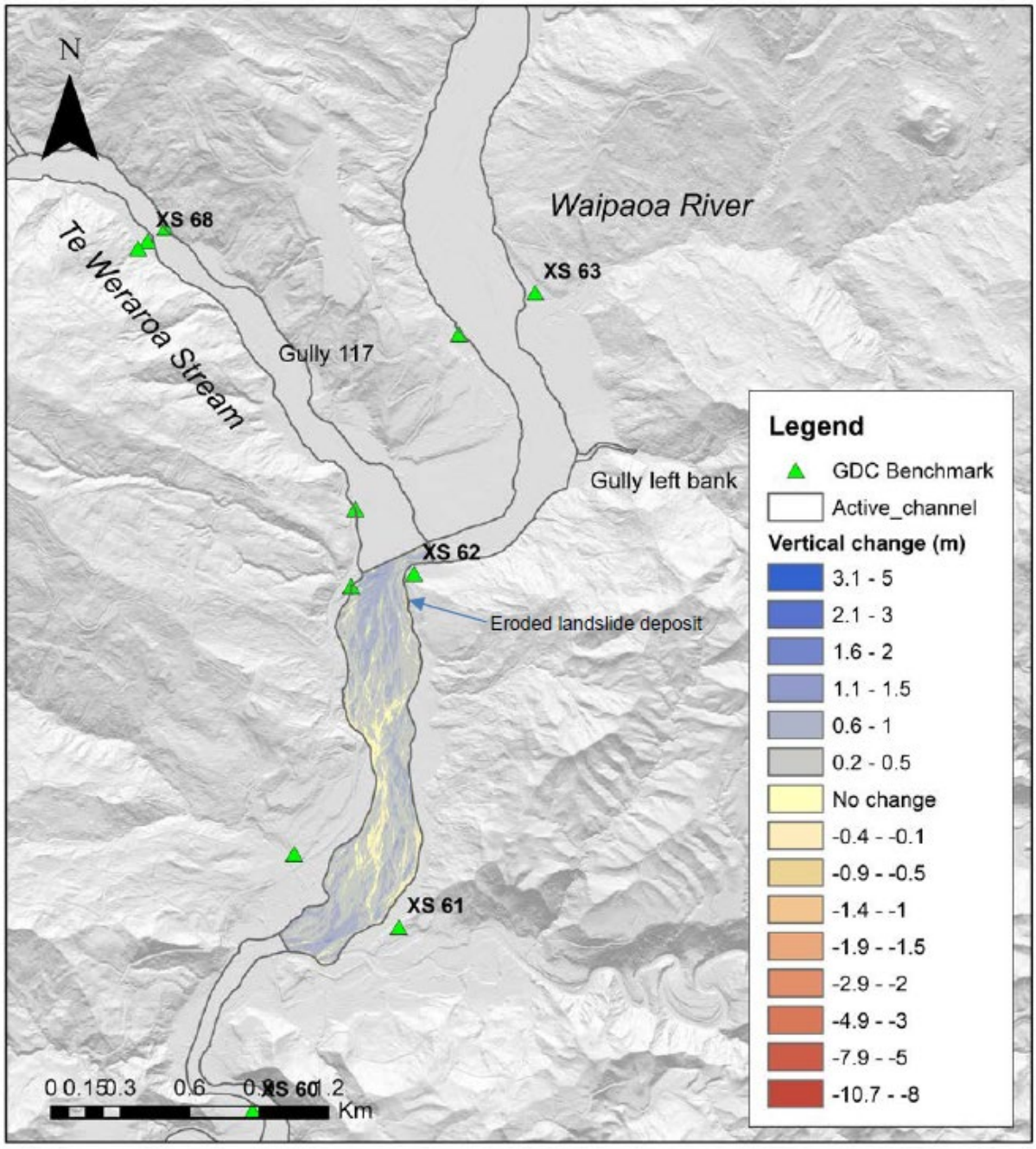

Figure A1.3 LiDAR digital elevation model of difference showing the vertical elevation change (in metres) for the Waipaoa River upstream of the gorge reach.

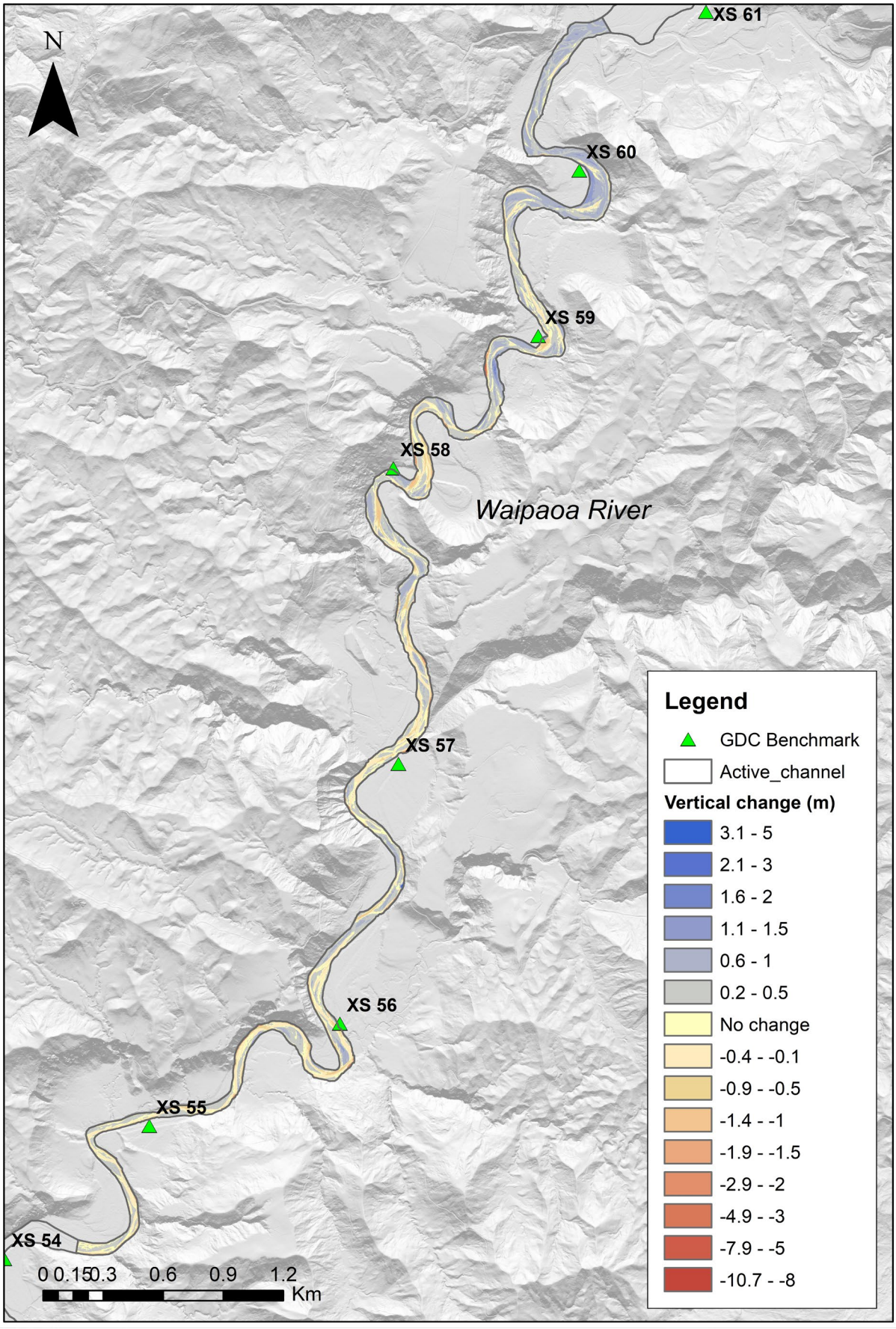

Figure A1.4 LiDAR digital elevation model of difference showing the vertical elevation change (in metres) for the upper gorge reach.

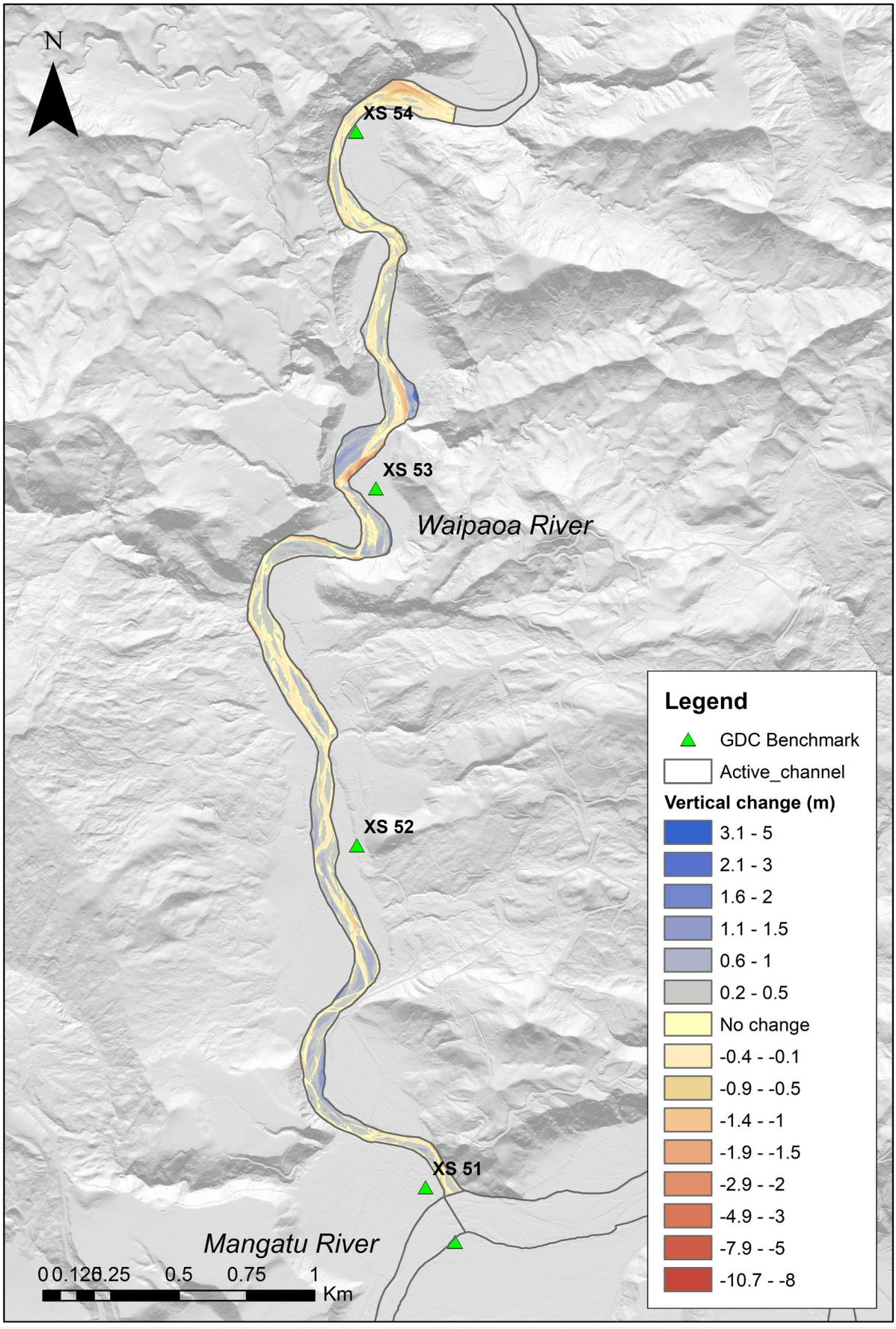

Figure A1.5 LiDAR digital elevation model of difference showing the vertical elevation change (in metres) for the lower gorge reach.

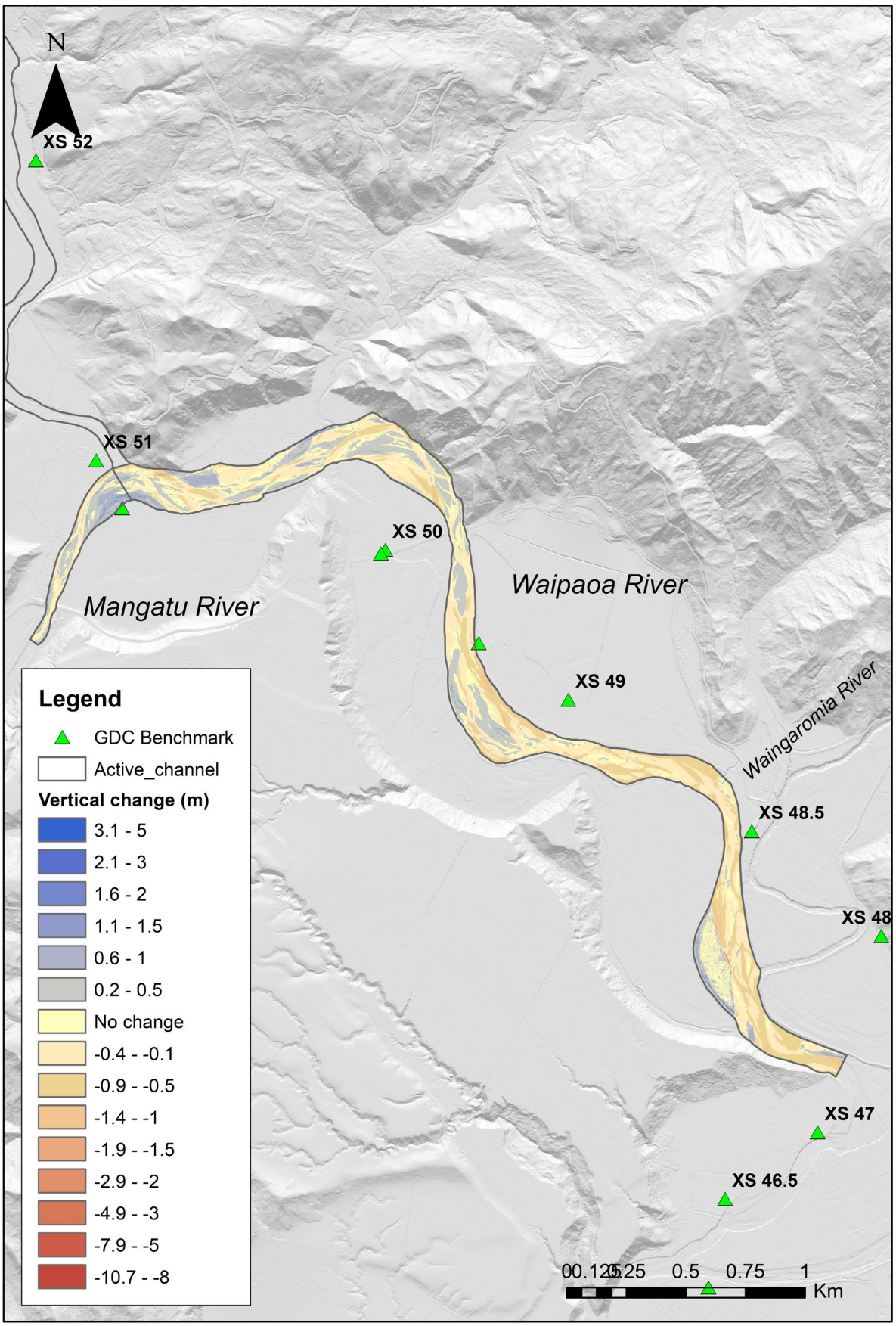

Figure A1.6 LiDAR digital elevation model of difference showing the vertical elevation change (in metres) for the Waipaoa River downstream of gorge and Mangatu River reaches.

APPENDIX 2 GISBORNE DISTRICT COUNCIL CROSS-SECTION SURVEY DATA

Table A2.1 Waipaoa River cross-section data used for volume calculations.

Survey Date	XS	Left Marker	Right Marker	MBL	Width (m)	Period	MBL2–MBL1	Average Width	XS Area	Average XS Area	Distance between XS	Volume*
26/05/2005	61	65.95	389.05	159.844	323.1	03-05	0.17	341.75	58.537	58.537	1570	91903
4/04/2007	61	65.98	392.61	159.827	326.63	05-07	-0.02	324.87	-5.670	-5.670	1570	-8903
25/06/2009	61	66.56	388.84	159.775	322.28	07-09	-0.05	324.46	-16.904	-16.904	1570	-26539
25/02/2010	61	65.2	387.7	159.867	322.57	09-10	0.09	322.43	29.683	29.683	1570	46602
4/03/2014	61	68.3	388.7	159.916	320.39	10-14	0.05	321.48	15.938	15.938	1570	25023
8/05/2019	61	68.0	388.0	159.991	320	14-19	0.07	320.20	23.942	23.942	1570	37588
26/05/2005	62A	8.6	223.3	170.628	214.66	04_05	-1.29	137.51	-177.742	-91.706	1680	-154066
11/04/2007	62A	8.6	250.8	170.670	242.19	05_07	0.04	228.43	9.729	-3.588	1680	-6027
25/06/2009	62A	8.3	247.7	170.626	239.47	07_09	-0.04	240.83	-10.678	9.502	1680	15964
25/02/2010	62A	8.3	247.3	170.656	238.97	09_10	0.03	239.22	7.341	11.639	1680	19554
4/03/2014	62A	8.3	249.8	170.846	241.48	10_14	0.19	240.23	45.471	34.706	1680	58307
7/05/2019	62A	2.2	244.0	170.843	241.85	14_19	0.00	241.67	-0.624	-0.312	1680	-525
26/05/2005	63	258.9	365.6	184.195	106.65	04_05	-0.05	104.27	-5.214	-91.478	1450	-132643
4/04/2007	63	244.7	367.1	184.399	122.4	05_07	0.20	114.53	23.454	16.591	1450	24058
25/06/2009	63	244.8	366.5	184.452	121.61	07_09	0.05	122.01	6.425	-2.127	1450	-3084
25/02/2010	63	275.8	365.8	184.318	90.02	09_10	-0.13	105.82	-14.145	-3.402	1450	-4933
4/03/2014	63	248.0	368.3	184.730	120.3	10_14	0.41	105.16	43.318	44.395	1450	64372
7/05/2019	63	248.0	364.0	184.790	116	14_19	0.06	118.15	7.028	3.202	1450	4643
26/05/2005	64	224.4	378.2	201.439	153.75	04_05	0.08	139.78	11.403	3.094	1590	4920
4/04/2007	64	197.8	372.0	201.470	174.17	05_07	0.03	163.96	5.054	14.254	1590	22664

Survey Date	XS	Left Marker	Right Marker	MBL	Width (m)	Period	MBL2–MBL1	Average Width	XS Area	Average XS Area	Distance between XS	Volume*
25/06/2009	64	240.5	375.5	201.188	135.04	07_09	-0.28	154.61	-43.542	-18.559	1590	-29508
25/02/2010	64	214.8	376.2	201.178	161.39	09_10	-0.01	148.22	-1.500	-7.823	1590	-12438
4/03/2014	64	299.6	374.7	200.601	75.07	10_14	-0.58	118.23	-68.239	-12.461	1590	-19813
7/05/2019	64	242.0	370.0	200.373	128	14_19	-0.23	101.54	-23.197	-8.084	1590	-12854
26/05/2005	65	12.2	213.3	218.52	201.17	04_05	-0.06	201.13	-12.625	-0.611	1580	-965
4/04/2007	65	1.1	213.6	218.43	212.49	05_07	-0.10	206.83	-19.874	-7.410	1580	-11708
25/06/2009	65	1.1	211.6	218.31	210.54	07_09	-0.11	211.52	-23.797	-33.669	1580	-53198
25/02/2010	65	46.6	180.4	218.10	133.79	09_10	-0.21	172.17	-36.389	-18.945	1580	-29933
4/03/2014	65	39.7	211.3	217.88	171.69	10_14	-0.23	152.74	-34.631	-51.435	1580	-81268
7/05/2019	65	27.0	216.0	217.60	189	14_19	-0.28	180.35	-50.382	-36.789	1580	-58127
26/05/2005	66	46.0	132.2	234.84	86.20	04_05	-0.08	83.12	-6.828	-9.726	1630	-15854
4/04/2007	66	28.5	137.2	235.11	108.64	05_07	0.27	97.42	26.723	3.425	1630	5582
25/06/2009	66	29.4	137.7	234.63	108.32	07_09	-0.48	108.48	-52.247	-38.022	1630	-61976
19/03/2010	66	15.8	137.7	235.00	121.92	09_10	0.37	115.12	42.736	3.174	1630	5173
7/03/2014	66	15.6	135.9	234.75	120.27	10_14	-0.25	121.10	-30.454	-32.543	1630	-53045
7/05/2019	66	17.0	119.0	234.20	102.00	14_19	-0.55	111.14	-60.760	-55.571	1630	-90581
26/05/2005	67	29.8	71.9	253.614	42.1	04_05	0.04	42.43	1.621	-2.603	1680	-4374
4/04/2007	67	26.4	102.5	254.799	76.11	05_07	1.18	59.11	70.027	48.375	1680	81271
25/06/2009	67	26.2	101.6	254.702	75.4	07_09	-0.10	75.76	-7.314	-29.780	1680	-50031
19/03/2010	67	20.2	102.5	254.416	82.29	09_10	-0.29	78.85	-22.512	10.112	1680	16989
7/03/2014	67	20.4	101.4	254.102	81.01	10_14	-0.31	81.65	-25.640	-28.047	1680	-47119
7/05/2019	67	68.0	102.0	253.843	34	14_19	-0.26	57.51	-14.942	-37.851	1680	-63589

* Change in volume between successive cross-sections.

Table A2.2 Te Weraroa Stream cross-section data used for volume calculations.

Survey Date	XS	Left Marker	Right Marker	MBL	Width (m)	Period	MBL2–MBL1	Average Width	XS Area	Average XS Area	Distance between XS	Change in Volume*
9/06/2005	68	27.61	88.41	205.768	60.8	-	-	-	-	-	-	-
11/04/2007	68	27.41	89.02	205.883	61.61	05-07	0.115	61.21	7.035	7.035	1670	-
7/03/2014	68	27.79	88.98	205.560	61.19	07-14	-0.323	61.40	-19.835	-19.835	1670	-
6/05/2019	68	27.61	87.74	205.335	60.13	14-19	-0.225	60.66	-13.642	-13.642	1670	-
9/06/2005	69	7.08	151.63	235.231	144.55	-	-	-	-	-	-	-
11/04/2007	69	6.87	156.31	235.132	149.44	05-07	-0.099	147.00	-14.567	-3.766	1529	-5,758
7/03/2014	69	6.61	152.32	234.615	145.71	07-14	-0.517	147.58	-76.294	-48.064	1529	-73,490
6/05/2019	69	7.19	152.22	234.249	145.03	14-19	-0.366	145.37	-53.217	-33.430	1529	-51,114
6/06/2005	70	13.75	177.17	272.762	163.42	-	-	-	-	-	-	-
11/04/2007	70	7.25	177.89	272.589	170.64	05-07	-0.173	167.03	-28.930	-21.748	1227	-26,685
7/03/2014	70	7.91	180.9	271.940	172.99	07-14	-0.650	171.82	-111.602	-93.948	1227	-115,274
6/05/2019	70	52.9	176.85	271.267	123.95	14-19	-0.673	148.47	-99.888	-76.553	1227	-93,930
9/06/2005	71	7.49	214.9	302.936	207.41	-	-	-	-	-	-	-
11/04/2007	71	7.55	215.12	302.558	207.57	05-07	-0.378	207.49	-78.523	-53.727	1564	-84,028
7/03/2014	71	101.69	214.11	300.639	112.42	07-14	-1.918	160.00	-306.928	-209.265	1564	-327,290
6/05/2019	71	149.08	215.41	298.267	66.33	14-19	-2.372	89.38	-211.976	-155.932	1564	-243,878
										Net Volume Change		-1,021,447

* Change in volume between successive cross-sections.

www.gns.cri.nz

Principal Location

1 Fairway Drive, Avalon
Lower Hutt 5010
PO Box 30368
Lower Hutt 5040
New Zealand
T +64-4-570 1444
F +64-4-570 4600

Other Locations

Dunedin Research Centre
764 Cumberland Street
Private Bag 1930
Dunedin 9054
New Zealand
T +64-3-477 4050
F +64-3-477 5232

Wairakei Research Centre
114 Karetoto Road
Private Bag 2000
Taupo 3352
New Zealand
T +64-7-374 8211
F +64-7-374 8199

National Isotope Centre
30 Gracefield Road
PO Box 30368
Lower Hutt 5040
New Zealand
T +64-4-570 1444
F +64-4-570 4657